SUPPORTING INFORMATION

A Highly Anisotropic Family of Hexagonal Bipyramidal Dy(III) Unsaturated 18-Crown-6 Complexes Exceeding Blockade Barrier over 2700K: A Computational Exploration

*Shruti Moorthy, Ibtesham Tarannum[§], Kusum Kumari[§] and Saurabh Kumar Singh**

Department of Chemistry, Indian Institute of Technology, Hyderabad Kandi, Sangareddy, Telangana, India, 502284
E-mail: sksingh@chy.iith.ac.in

[§]authors contributed equally

SUPPORTING INFORMATION

Table of Contents

SUPPORTING INFORMATION

SUPPORTING INFORMATION

SUPPORTING INFORMATION

Computational Details

1. Geometry Optimization:

The gas phase geometry optimizations were carried out using ORCA 5.0.3[1] code at the BP86 level of theory for all the mononuclear complexes [2,3]. The dispersion corrections were accounted for by using Grimme's dispersion with Becke-Johnson (D3BJ) method incorporated in ORCA.[4] The BP86 level of theory has been robust in the geometry optimization of mononuclear lanthanide and actinide complexes.[5–8] For the Dy atom, core electrons were replaced by def2-ECP pseudopotential (for 28 core electrons, l_{max}=5), while TZVP were used to treat the valence electrons. For O, S, Se, F, Cl, Br, we have used the def2-TZVP basis set, while Sapporo-TZP basis sets were used for the I atom.[9] For all the C and H atoms, we have used the def2-SVP basis set.[10] Vibrational frequency calculations show no negative frequency, thus confirming the stationary point as the local minima. A very tight SCF ($1 \times 10^{-8} E_h$) criterion was chosen for energy minimization. The "*slowconv*" and "*KDIIS*" criteria and large integration grid settings (GRID9 for Dy) were turned on throughout the calculations for smooth convergence.

To assess the reliability of our computational methodology in predicting the structural parameters, we have optimized twelve different mononuclear Dy(III) complexes for which the X-ray crystal structure is reported. DFT-optimized geometry nicely reproduces the X-ray structural parameters (see the overlay of experimental and DFT-optimized geometry in Scheme S1(a)). One-to-one comparison of relevant bond lengths (Dy-ligand) and bond angles between the DFT optimized and X-ray structure shows a near-linear correlation with an R-value and slope value of 0.92-0.95, highlighting the robustness of our computational methodology in predicting the structures.(see Scheme S1 (b) and (c)

SUPPORTING INFORMATION

(a)

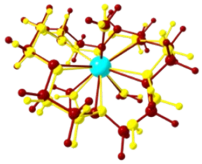

1
Inorg. Chem., 2018, 57, 13225–13234

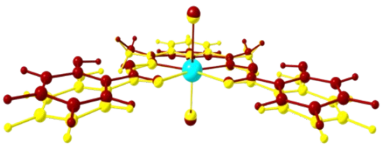

2
Dalton Trans., 2023, 52, 2804–2815

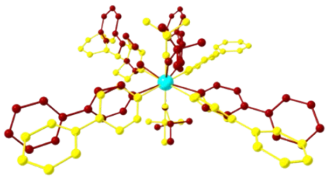

3
Chem. – Eur. J., 2021, 27, 2623–2627

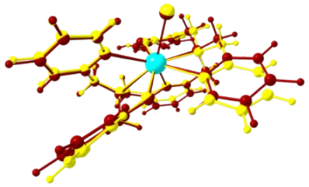

4
Inorg. Chem. Front., 2021, 8, 2349–2355

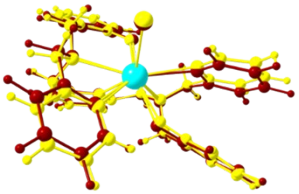

5
Inorg. Chem. Front., 2021, 8, 2349–2355

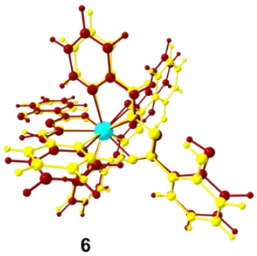

6
Inorg. Chem. Front., 2020, 7, 4805

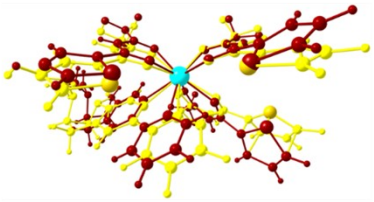

7
Inorg. Chem. 2010, 49, 969–976

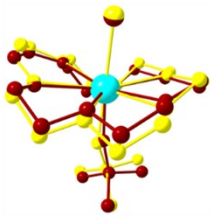

8
Inorg. Chem. 2022, 61, 227–235

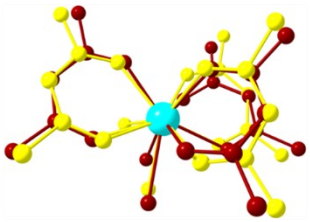

9
Angew. Chem. Int. Ed., 2010, 49, 7448–7451

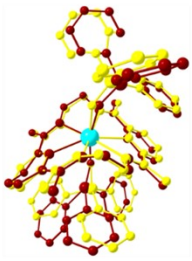

10
Angew. Chem. Int. Ed., 2019, **58**, 14146–14151

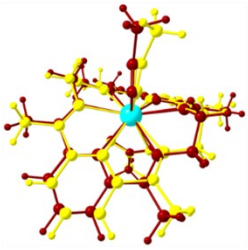

11
Angew. Chem. Int. Ed., 2019, **58**, 14146–14151

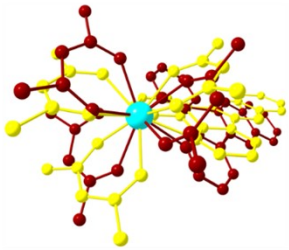

12
Chem. – Eur. J., 2012, **18**, 2484–2487

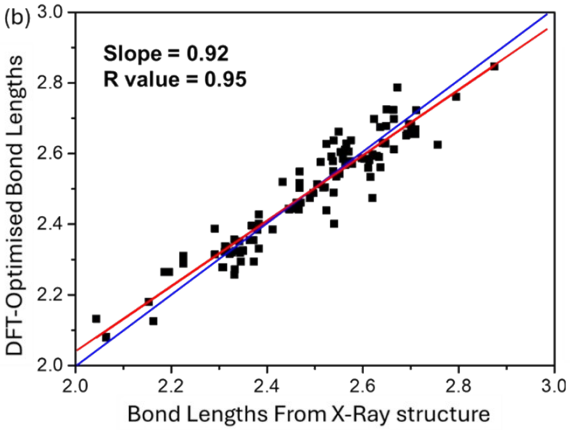

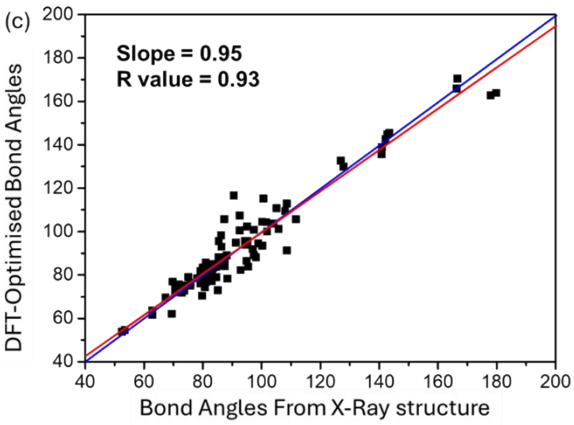

SUPPORTING INFORMATION

Scheme 1. (a) Overlay plots of the X-ray crystal structure (in red) and the DFT-optimised structures (in yellow) (b) Correlation between the bond lengths in DFT optimised and X-Ray crystal structure in a series of Dy(III) complexes; (c) Correlation between the bond angles in DFT optimised and X-Ray crystal structure in a series of Dy(III) complexes The red line represents the linear fit obtained between the DFT optimised and crystal structure values, while the blue line represents the ideal 1:1 correspondence between the experimental and computed values.

Conformational Search

First, we have performed the conformational search analysis using the xTB CREST4 code.[11] The key procedure implemented in CREST is a conformational search workflow abbreviated as iMTD-GC. The iMTD-GC workflow generates conformer/rotamer ensembles (CREs) by extensive meta-dynamic sampling (MTD) based on an additional genetic z-matrix crossing (GC) step at the end. CRE is the thermally accessible ensemble of minimum-energy structures consisting of conformers as well as rotamers. The conformational search was carried out in an energy window of ~ 10kJ/mole. Here, we have carried out CREST calculations on eleven mononuclear Dy(III) complexes with the general formula $[Dy(U18C6)X_2]^+$ (where U18C6 = $[C_{12}H_{12}O_6]$ (**1**), $[C_{12}H_{12}S_6]$ (**2**), $[C_{12}H_{12}Se_6]$ (**3**), $[C_{12}H_{12}O_4S_2]$ (**4**), $[C_{12}H_{12}O_4Se_2]$ (**5**) and X= F, Cl, Br, I as an axial ligand) and the saturated analogue of $\mathbf{1_{Cl}}$. Conformational analysis of $\{DyX_2\}$ encapsulated in the unsaturated 18-crow-6 ligands yields a single conformer for all the complexes $\mathbf{1_X}$-$\mathbf{5_X}$. In all the eleven complexes, we observed that the unsaturated 18-crown-6 ligand occupies the equatorial positions while the X atoms occupy the axial position, resulting in a hexagonal bipyramidal geometry around the Dy(III) ion. Contrarily, we observed 14 different conformers for the saturated analogue of the $\mathbf{1_{Cl}}$ $[Dy(18C6)Cl_2]^+$ analogue within the ~10 kJ/mol. All the obtained conformers were optimized at the DFT level of theory to find the lowest energy structure.

2. Energy Decomposition Analysis and ETS-NOCV Analysis:

To further understand the nature of bonding in all the eleven complexes and the saturated analogue of $\mathbf{1_{Cl}}$, we have carried out an energy decomposition analysis (EDA) using the ADF 2021 code. All these calculations were carried out in a scalar relativistic framework using hybrid PBE0 functional[12], where scalar relativistic effects were modelled by zeroth-order relativistic approximation (ZORA) as implemented in ADF.

[13] Slater-type all electron TZP basis set for Dy atom and DZP basis set for the remaining atoms, with "*no frozen core*" approximation. Grimme's D3 empirical corrections with Becke–Johnson damping (D3BJ) were applied to incorporate dispersion corrections. [4] All these calculations were conducted in the gas phase. Natural Bonding Orbital (NBO) analysis has been carried out using Weinhold's NBO 6.0 code implemented in the ADF 2021 code to assess the natural population analysis and bonding interactions.[13]

3. Magnetic Anisotropy and Ab Initio Ligand Field Theory Calculations

Complete-active space self-consistent field (CASSCF) calculations[14] were performed on DFT-optimized lowest energy structures of all the complexes to assess the magnetic properties. For these calculations, we employed DKH-adapted def2-TZVP for O, S, Se, F, Cl, Br, Sapporo-DKH-TZP for the I atom [9] and all-electron SARC-DKH-TZVP basis set for Dy(III) centre.[15] The Dy(III) ion has a $^6H_{15/2}$ ground state with an f^9 configuration, and we have constructed an active space of nine active electrons in seven active 4*f* – orbitals, i.e. CAS(9,7). Using this active space, we have computed 21 sextets and 224 quartets and performed the spin-orbit calculations using the spin–orbit mean field (SOMF-IX) operator and second-order Douglas–Kroll–Hess (DKH2) method. The computed spin-free energy and spin-orbit energies are provided in Table S14-S19. Ab initio ligand field theory (AILFT) calculations were performed at the CASSCF levels of theory to estimate the interelectronic repulsion in terms of Slater–Condon parameters and one electron energies to represent the *f*-orbital splitting.[16] Next, we used standalone SINGLE_ANISO module code to extract the g-values of the low-lying Kramer doublets, crystal field parameters, wave function decomposition analysis and constructed the *ab-initio blockage barrier* by computing the transverse magnetic moment between each KD, which gives us the probability of magnetic relaxation from a given KD.

Effective energy demagnetization barrier (U_{eff})

We have computed the effective energy demagnetization barriers U_{eff} for the Orbach relaxation process, using the method previously published by Aravena et al., in ref [17], which utilize the energy of the eight Kramer's doublets and the magnetic transition dipole moment related to the transition between the respective KDs (i.e. +1 → – 1) from the CAS(9,7) calculations. This method involves the use of the following formula,

SUPPORTING INFORMATION

$$U_{eff}(T) = \sum_{i=1}^{M} \frac{k_i(T)}{N_k} E_i$$

Here, M denotes the number of KDs, k_i denotes the demagnetization rates of the KDs of energies E_i, N_k a normalization factor for k_i.

$$k_i(T) = \frac{\exp\left(-\frac{\varepsilon}{k_B T}\right)}{Z} k_{QT,i}$$

k_B is the Boltzmann constant, $k_{QT,i}$ represent the magnetic transition dipole moment and T and Z are the temperature and the partition function, respectively. The computed U_{eff} values are tabulated in Table 1. As proposed earlier by Aravena et al.,[18] the blocking temperatures can be estimated by dividing the computed energy barrier by a factor of 28, which nicely correlates with the experimental values quite well. The blocking temperatures reported in Table 1 are estimated using this approach.

SUPPORTING INFORMATION

Table S1: Selected structural parameters of complexes $\mathbf{1_X}$-$\mathbf{5_X}$.

Complex	Label	Avg. Dy-L_{eq} (Å)	Avg. Dy-X (Å)	∠X-Dy-X (°)
$[Dy(C_2H_2O)_6F_2]^+$	$\mathbf{1_F}$	2.673	2.029	150.2
$[Dy(C_2H_2O)_6Cl_2]^+$	$\mathbf{1_{Cl}}$	2.641	2.507	162.9
$[Dy(C_2H_2O)_6Br_2]^+$	$\mathbf{1_{Br}}$	2.639	2.670	163.4
$[Dy(C_2H_2O)_6I_2]^+$	$\mathbf{1_I}$	2.630	2.896	167.4
$[Dy(C_2H_2S)_6F_2]^+$	$\mathbf{2_F}$	3.185	2.031	150.6
$[Dy(C_2H_2S)_6Cl_2]^+$	$\mathbf{2_{Cl}}$	3.167	2.541	174.1
$[Dy(C_2H_2S)_6Br_2]^+$	$\mathbf{2_{Br}}$	3.162	2.695	179.8
$[Dy(C_2H_2S)_6I_2]^+$	$\mathbf{2_I}$	3.155	2.912	179.9
$[Dy(C_2H_2Se)_6Cl_2]^+$	$\mathbf{3_{Cl}}$	3.335	2.542	169.2
$[Dy(C_{12}H_{12}S_2O_4)Cl_2]^+$	$\mathbf{4_{Cl}}$	2.970(S) / 2.802(O)	2.552	152.5
$[Dy(C_{12}H_{12}Se_2O_4)Cl_2]^+$	$\mathbf{5_{Cl}}$	3.103(Se) / 2.777(O)	2.512	156.4

Table S2: DFT optimized low-lying conformers of the $[Dy(18C6)Cl_2]^+$ along with their absolute SCF electronic energy, enthalpy (H) and Gibbs free energy (G)

Conformer	SCF Electronic Energy (kcal/mol)	H (kcal/mol)	G (kcal/mol)
1	-2728.302	-2728.301	-2728.381
2	**-2728.310**	**-2728.309**	**-2728.389**
3	-2728.306	-2728.305	-2728.383
4	-2728.305	-2728.304	-2728.383
5	-2728.310	-2728.309	-2728.387
6	-2728.307	-2728.306	-2728.385
7	-2728.306	-2728.305	-2728.383
8	-2728.310	-2728.309	-2728.388
9	-2728.310	-2728.309	-2728.387
10	-2728.307	-2728.306	-2728.384
11	-2728.306	-2728.305	-2728.383
12	-2728.309	-2728.308	-2728.387
13	-2728.309	-2728.308	-2728.387
14	-2728.306	-2728.305	-2728.381

the lowest energy conformer has been made bold

SUPPORTING INFORMATION

Table S3: Continuous Shape Measure (CShM) analysis for Dy(III) ions in complexes $\mathbf{1_X}$-$\mathbf{5_X}$

	OP-8	HPY-8	**HBPY-8**	CU-8	SAPR-8	TDD-8	JGBF-8	JETBPY-8	JBTPR-8	BTPR-8	JSD-8	TT-8	ETBPY-8
$\mathbf{1_F}$	30.148	16.958	**2.314**	11.040	17.946	15.530	9.924	23.882	16.969	16.750	17.292	11.831	22.050
$\mathbf{1_{Cl}}$	30.782	19.578	**0.756**	9.093	16.184	13.840	8.543	24.234	15.772	15.095	16.221	9.875	20.645
$\mathbf{1_{Br}}$	31.198	20.135	**0.697**	8.913	16.014	13.648	8.906	24.635	15.828	14.952	16.503	9.697	20.598
$\mathbf{1_{I}}$	32.042	21.832	**0.753**	8.760	16.129	13.586	9.167	25.698	16.145	15.011	17.176	9.584	21.235
$\mathbf{2_F}$	29.323	17.753	**3.825**	12.713	19.959	17.728	11.749	24.762	18.542	18.932	18.559	13.269	23.842
$\mathbf{2_{Cl}}$	30.254	20.772	**0.918**	9.655	18.836	16.164	10.506	25.489	17.975	17.737	18.693	10.280	23.447
$\mathbf{2_{Br}}$	31.127	21.843	**0.474**	9.132	18.926	16.217	10.337	26.143	18.317	17.948	18.986	9.815	23.827
$\mathbf{2_{I}}$	31.692	22.466	**0.146**	8.686	18.622	15.866	10.558	26.510	18.276	17.682	19.131	9.383	23.671
$\mathbf{3_{Cl}}$	29.771	19.921	**1.472**	10.226	19.002	16.471	10.684	25.188	17.800	17.752	18.537	10.691	23.476
$\mathbf{4_{Cl}}$	28.908	16.854	**3.279**	11.636	15.825	14.183	6.721	22.080	14.520	13.504	13.888	12.384	18.073
$\mathbf{5_{Cl}}$	29.207	17.586	**3.248**	11.605	15.971	14.416	6.331	22.798	14.623	13.981	13.852	12.339	18.458
Determined Geometry: HBPY-8													

OP-8, D_{8h}, Octagon; HPY-8, C_{7v}, Heptagonal pyramid; HBPY-8, D_{6h}, Hexagonal bipyramid; CU-8, O_h, Cube; SAPR-8, D_{4d}, Square antiprism; TDD-8, D_{2d},Triangular dodecahedron; JGBF-8, D_{2d}, Johnson gyrobifastigium J26; JETBPY-8, D_{3h}, Johnson elongated triangular bipyramid J14; JBTPR8, C_{2v}, Biaugmented trigonal prism J50; BTPR-8, C_{2v}, Biaugmented trigonal prism; JSD-8, D2d, Snub diphenoid J84; TT-8, T_d , Triakis tetrahedron; ETBPY-8, D_{3h}, Elongated trigonal bipyramid.

SUPPORTING INFORMATION

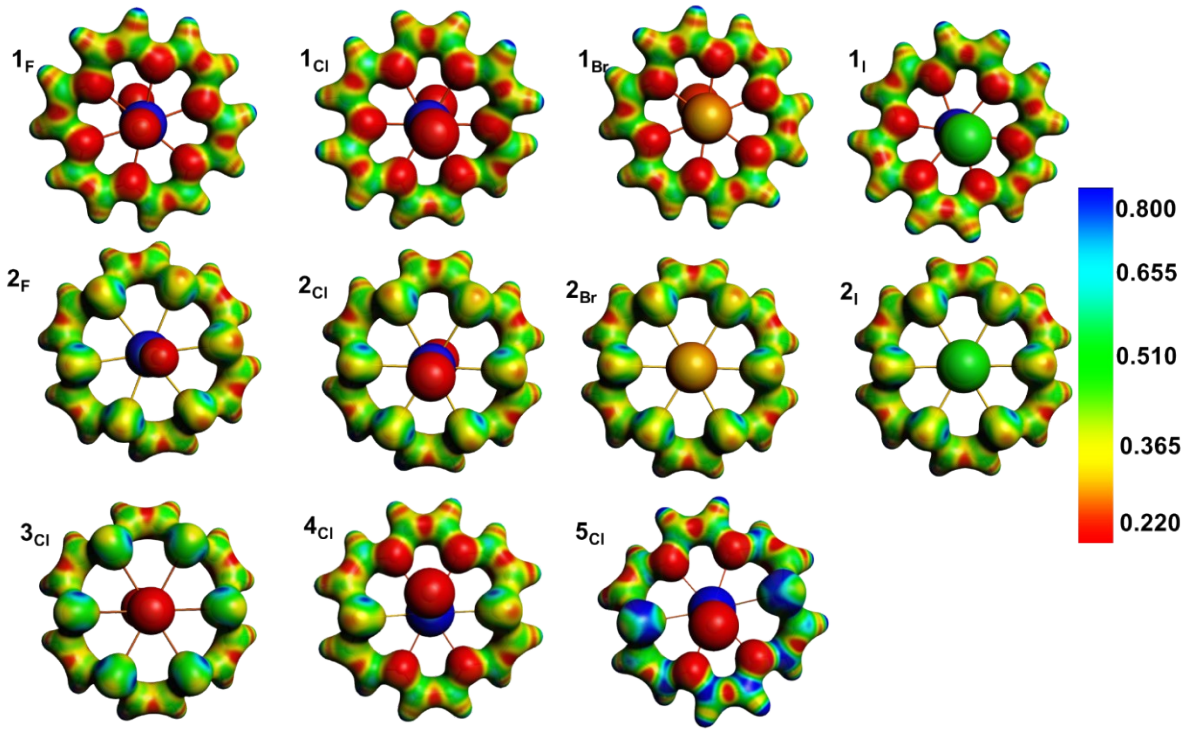

Figure S1: Molecular Electrostatic Maps/(MEP) plots for complexes $\mathbf{1_X}$-$\mathbf{5_X}$. The red and blue colours represent the most electronegative and electropositive regions, respectively.

Energy Decomposition Analysis

Energy Decomposition analysis was carried out on all the complexes of $\mathbf{1_X}$-$\mathbf{5_X}$ to understand the nature of interaction bonding interaction by preparing the two fragments {DyX_2} and the {U18C6}. The total interaction energy (ΔE_{int}) of a complex can be defined as the difference in energies between the complex and individual fragments as $\Delta E_{int} = E_{complex} - (E_{DyX2} + E_{U18C6})$, which can be further decomposed in terms of electrostatic interaction, Pauli repulsion, orbital interactions, and dispersion interaction energies as follows:

$$\Delta E_{int} = \Delta E_{Elstat} + \Delta E_{pauli} + \Delta E_{orbital} + \Delta E_{disp}$$

where the term ΔE_{Elstat} corresponds to the electrostatic interaction between metal and ligands (which is attractive in nature), ΔE_{Pauli} refers to the Pauli repulsion energy, $\Delta E_{orbital}$ accounts for orbital interactions resulting from electron pair bonding, charge transfer and polarization terms, and ΔE_{disp} represents the dispersion interaction terms. Fig. S2 and Tables S4-S5 show the trend in the binding energy for all eleven complexes. EDA analysis predicts the following trend in the ΔE_{int} value for $\mathbf{1_X}$ series $\mathbf{1_F} < \mathbf{1_{Cl}} \sim \mathbf{1_{Br}} \sim \mathbf{1_I}$ and for $\mathbf{2_X}$:

$\mathbf{2_F} < \mathbf{2_{Cl}} \sim \mathbf{2_{Br}} \sim \mathbf{2_I}$, with the $\mathbf{1_X}$ series complexes lower binding energy compared to $\mathbf{2_X}$ family of complexes. Within each series, we can see that the -F analogue has the lowest ΔE_{int} value, while the -Cl, -Br and -I analogues have nearly the same values. In both the $\mathbf{1_X}$ and $\mathbf{2_X}$ families of complexes, the decomposed energies show that the electrostatic and orbital interactions sharply increase as we move from -F to -Cl analogues and remain constant for heavier halides. In the $\mathbf{1_X}$ family of complexes, we have noticed that the most significant contribution to binding energy emerges from the electrostatic interactions, which nearly contribute ~70% of the total binding energy, followed by orbital interactions contributing ~62% of the total binding energy. On the other hand, as we move $\mathbf{1_X}$-$\mathbf{2_X}$ complexes, we observed that orbital interaction dominates electrostatic interactions and contributes ~75% of the total binding energy compared to the ~60% contribution from the electrostatic interactions. As we move from oxa to the thia crown complexes, the electrostatic interaction decreases significantly due to a decrease in the electronegativity as we move down from O to S/Se atom (see Fig S1). Contrarily, the strength of the orbital interaction marginally increases as we move from O to S/Se, which is rooted back to weak lanthanide-ligand covalency. In all the studied complexes, the Pauli interactions are always positive, and we observed a following trend in the ΔE_{Pauli} value: I > Br > Cl > F. Finally, the dispersion interaction stabilises all complexes by ~8 to 15 kcal mol^{-1}, contributing <10% of the total binding energy.

Table S4: EDA analysis for complexes $\mathbf{1_X}$-$\mathbf{5_X}$. All the values provided here are in the kcal/mol.

Complexes	E_{Pauli}	E_{Elstat}	E_{Orb}	E_{Disp}	E_{Int}	%Covalency
$\mathbf{1_F}$	48.1	-94.6	-83.1	-8.5	-138.1	46.7
$\mathbf{1_{Cl}}$	60.7	-106.2	-99.6	-11.6	-156.6	48.4
$\mathbf{1_{Br}}$	65.7	-108.1	-101.3	-12.7	-156.4	48.4
$\mathbf{1_I}$	77.1	-116.3	-102.1	-14.2	-155.5	46.8
$\mathbf{2_F}$	54.9	-72.6	-85.1	-10.4	-113.3	54.0
$\mathbf{2_{Cl}}$	62.1	-79.6	-104.9	-14.3	-136.8	56.9
$\mathbf{2_{Br}}$	66.0	-81.6	-106.0	-15.8	-137.4	56.5
$\mathbf{2_I}$	79.2	-91.3	-110.0	-17.9	-139.9	54.7
$\mathbf{3_{Cl}}$	58.0	-77.6	-107.3	-14.5	-141.4	58.0
$\mathbf{4_{Cl}}$	70.6	-99.4	-100.3	-12.7	-141.8	50.2
$\mathbf{5_{Cl}}$	58.0	-77.6	-107.3	-14.5	-141.4	58.0
$\mathbf{[Dy(18C6)Cl_2]^+}$	90.34	-164.31	-129.61	-13.86	-217.44	44.1

SUPPORTING INFORMATION

Table S5: Contribution (%) of decomposition energies to Total Binding Energy for complexes $\mathbf{1_X}$-$\mathbf{5_X}$.

Complexes	E_{Pauli} (%)	E_{Elstat} (%)	E_{Orb} (%)	E_{Disp} (%)
$\mathbf{1_F}$	-34.8	68.5	60.1	6.1
$\mathbf{1_{Cl}}$	-38.8	67.8	63.6	7.4
$\mathbf{1_{Br}}$	-42.0	69.1	64.8	8.1
$\mathbf{1_I}$	-49.5	74.8	65.7	9.1
$\mathbf{2_F}$	-48.4	64.1	75.1	9.2
$\mathbf{2_{Cl}}$	-45.4	58.2	76.7	10.5
$\mathbf{2_{Br}}$	-48.0	59.4	77.2	11.5
$\mathbf{2_I}$	-56.6	65.2	78.6	12.8
$\mathbf{3_{Cl}}$	-41.1	54.9	75.9	10.2
$\mathbf{4_{Cl}}$	-49.8	70.1	70.7	9.0
$\mathbf{5_{Cl}}$	-41.1	54.9	75.9	10.2
$[Dy(18C6)Cl_2]^+$	-41.5	75.6	59.6	6.4

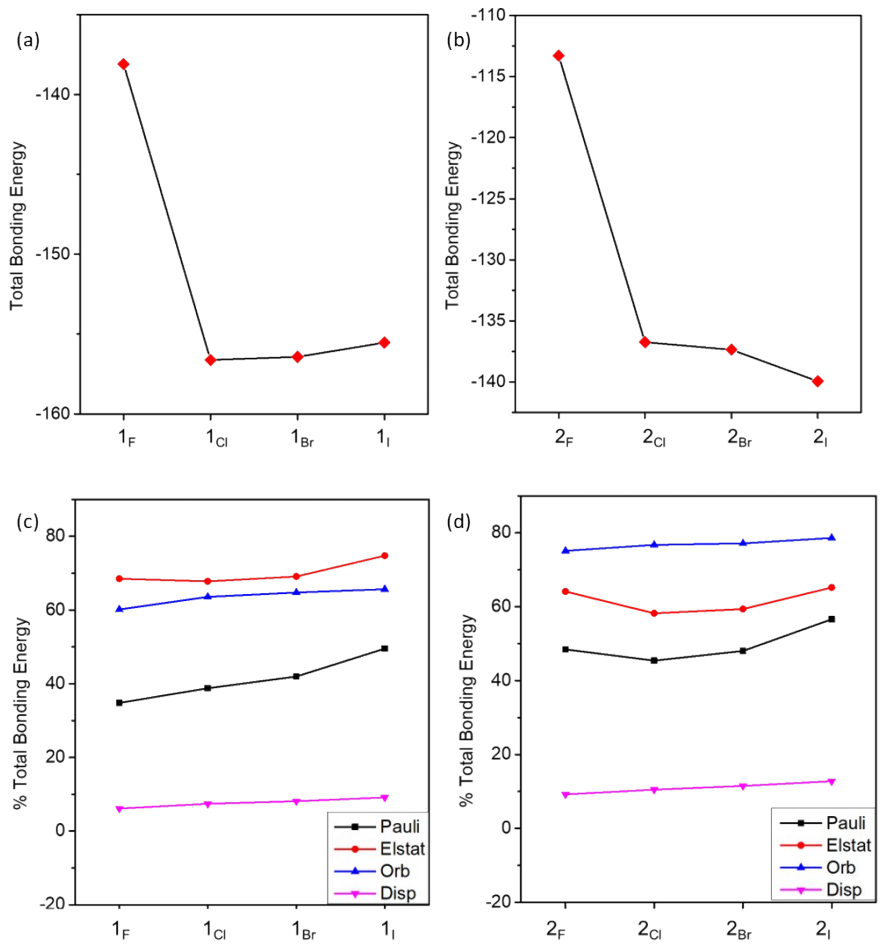

Figure S2: (a) and (b) DFT computed trends in the total binding energy; (c) and (d) the percentage contribution of the decomposition energies to the total binding energy for $\mathbf{1_X}$ and $\mathbf{2_X}$, respectively.

SUPPORTING INFORMATION

Table S6: The EDA-NOCV results of complexes $\mathbf{1_X}$-$\mathbf{2_X}$ with different electronic states of fragments at the PBE0- D3(BJ) level. All the values provided here are in the kcal/mol.

Energy	$\mathbf{1_F}$	$\mathbf{1_{Cl}}$	$\mathbf{1_{Br}}$	$\mathbf{1_I}$	$\mathbf{2_F}$	$\mathbf{2_{Cl}}$	$\mathbf{2_{Br}}$	$\mathbf{2_I}$
ΔE_{Pauli}	48.1	60.7	65.7	77.1	54.9	62.1	66.0	79.2
ΔE_{elstat}	-94.6	-106.2	-108.1	-116.3	-72.6	-79.6	-81.6	-91.3
ΔE_{orb}	-83.1	-99.6	-101.3	-102.1	-85.1	-104.9	-106.0	-110.0
ΔE_{disp}	-8.5	-11.6	-12.7	-14.2	-10.4	-14.3	-15.8	-17.9
ΔE_{int}	-138.1	-156.6	-156.4	-155.5	-113.3	-136.8	-137.4	-139.9
ETS-NOCV Decomposed Orbital Interaction Energies								
$\Delta E_{orb(1)}$	-5.5	-6.5	-6.5	-6.4	-9.9	-11.4	-11.3	-11.6
$\Delta E_{orb(2)}$	-5.2	-6.6	-6.6	-6.0	-7.7	-9.8	-9.8	-10.1
$\Delta E_{orb(3)}$	-5.5	-6.1	-6.2	-5.8	-7.4	-9.9	-9.9	-9.9
Total ΔE_{orb}	-16.2	-19.2	-19.3	-18.2	-25.0	-31.1	-31.0	-31.6
Total ΔE_{orb} (as $\%E_{int}$)	11.8	12.2	12.4	11.7	22.0	22.8	22.6	22.6

Table S7: The shape of the first three highest electron deformation densities, $\Delta E_{orb(1)-(3)}$ at the PBE0-D3(BJ) level for complexes $\mathbf{1_X}$-$\mathbf{2_X}$. Isosurface values are 0.0002 au. The direction of the charge flow of the deformation densities is from red to blue. The ΔE_{orb} energies are in kcal/mol. The eigenvalues ν_i give the size of the charge migration.

Complex	$\Delta E_{orb(1)}$	$\Delta E_{orb(2)}$	$\Delta E_{orb(3)}$
$\mathbf{1_F}$	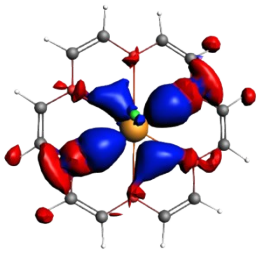 $\Delta\rho_{(1)}$ $\Delta E_{orb(1)}$ =-5.5; $\lvert\nu_1\rvert$=0.12	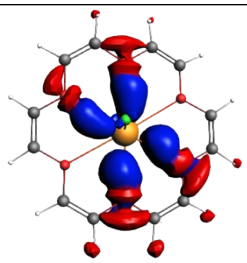 $\Delta\rho_{(2)}$ $\Delta E_{orb(2)}$ = -5.2; $\lvert\nu_2\rvert$=0.12	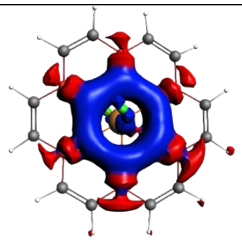 $\Delta\rho_{(3)}$ $\Delta E_{orb(3)}$ = -5.5; $\lvert\nu_2\rvert$=0.11
$\mathbf{1_{Cl}}$	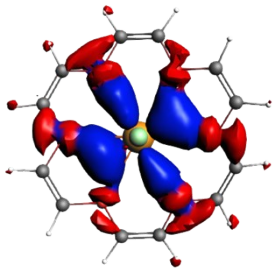 $\Delta\rho_{(1)}$ $\Delta E_{orb(1)}$ =-6.5; $\lvert\nu_1\rvert$ = 0.14	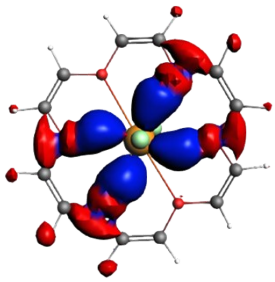 $\Delta\rho_{(2)}$ $\Delta E_{orb(2)}$ =-6.6; $\lvert\nu_1\rvert$ = 0.14	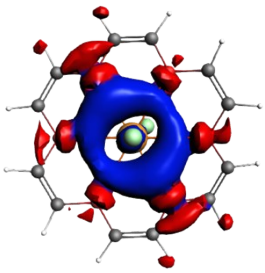 $\Delta\rho_{(3)}$ $\Delta E_{orb(3)}$ =-6.1; $\lvert\nu_1\rvert$ = 0.13

SUPPORTING INFORMATION

1_{Br}	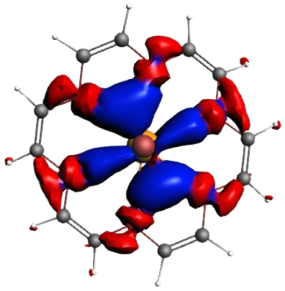 $\Delta\rho_{(1)}$ $\Delta E_{orb(1)}$ =-6.5; $\lvert\nu_1\rvert$ = 0.15	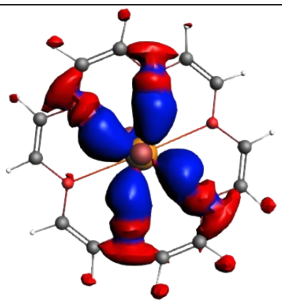 $\Delta\rho_{(2)}$ $\Delta E_{orb(2)}$ =-6.6; $\lvert\nu_1\rvert$ = 0.14	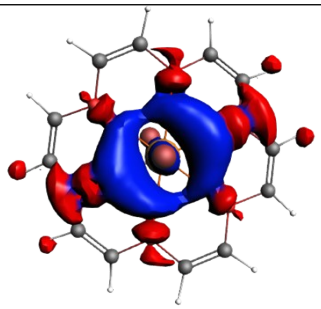 $\Delta\rho_{(3)}$ $\Delta E_{orb(3)}$ =-6.2; $\lvert\nu_1\rvert$ = 0.13
1_{I}	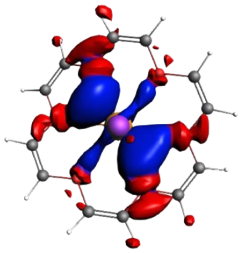 $\Delta\rho_{(1)}$ $\Delta E_{orb(1)}$ =-6.4; $\lvert\nu_1\rvert$ = 0.14	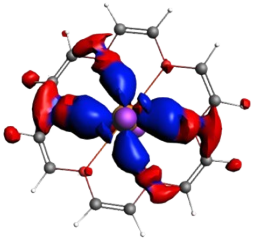 $\Delta\rho_{(2)}$ $\Delta E_{orb(2)}$ =-6.0; $\lvert\nu_1\rvert$ = 0.14	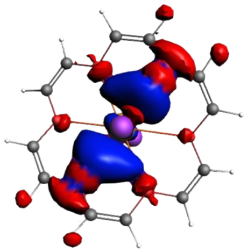 $\Delta\rho_{(3)}$ $\Delta E_{orb(3)}$ =-5.8; $\lvert\nu_1\rvert$ = 0.14
Interaction	[σ e^- donation 2p{**1**}→ 5d of Dy {DyF_2}]	[σ e^- donation 2p{**1**}→ 5d of Dy {DyX_2}]	[σe^- donation 2p{**1**}→ 6s of Dy {DyX_2}]
2_{F}	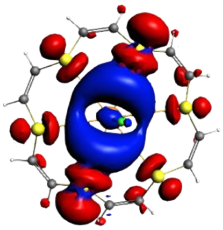 $\Delta\rho_{(1)}$ $\Delta E_{orb(1)}$ =-9.9; $\lvert\nu_1\rvert$ = 0.19	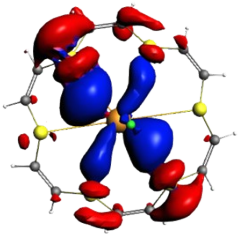 $\Delta\rho_{(2)}$ $\Delta E_{orb(2)}$ =-7.7; $\lvert\nu_1\rvert$ = 0.17	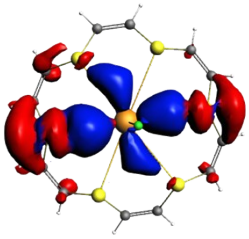 $\Delta\rho_{(3)}$ $\Delta E_{orb(3)}$ =-7.3; $\lvert\nu_1\rvert$ = 0.17
2_{Cl}	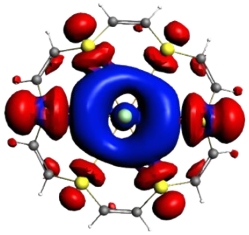 $\Delta\rho_{(1)}$ $\Delta E_{orb(1)}$ =-11.4; $\lvert\nu_1\rvert$ = 0.20	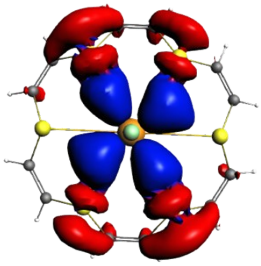 $\Delta\rho_{(2)}$ $\Delta E_{orb(2)}$ =-9.8; $\lvert\nu_1\rvert$ = 0.20	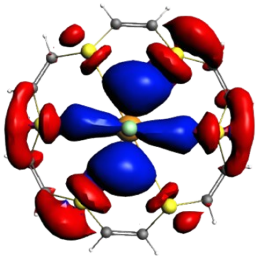 $\Delta\rho_{(3)}$ $\Delta E_{orb(3)}$ =-9.9; $\lvert\nu_1\rvert$ = 0.20
2_{Br}	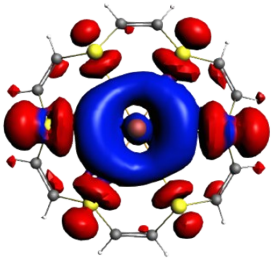 $\Delta\rho_{(1)}$ $\Delta E_{orb(1)}$ =-11.3; $\lvert\nu_1\rvert$ = 0.21	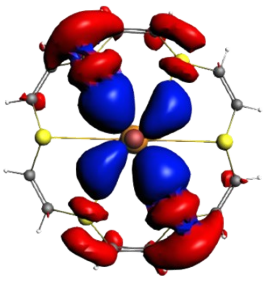 $\Delta\rho_{(2)}$ $\Delta E_{orb(2)}$ =-9.8; $\lvert\nu_1\rvert$ = 0.20	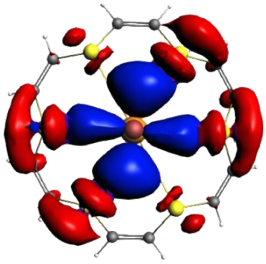 $\Delta\rho_{(3)}$ $\Delta E_{orb(3)}$ =-9.9; $\lvert\nu_1\rvert$ = 0.20

SUPPORTING INFORMATION

2_I	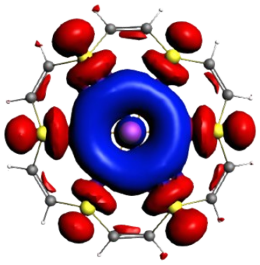 $\Delta\rho_{(1)}$ $\Delta E_{orb(1)}$ =-11.6; $\lvert\nu_1\rvert$ = 0.21	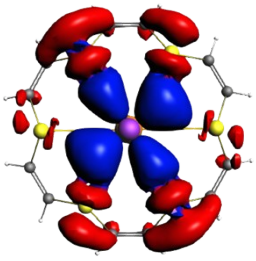 $\Delta\rho_{(2)}$ $\Delta E_{orb(2)}$ =-10.1; $\lvert\nu_1\rvert$ = 0.21	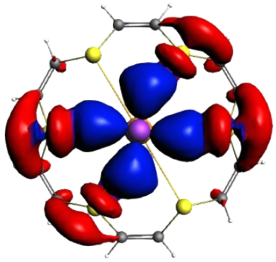 $\Delta\rho_{(3)}$ $\Delta E_{orb(3)}$ =-9.9; $\lvert\nu_1\rvert$ = 0.21
Interaction	[σ e^- donation 3p{**2**} →6s of Dy{DyX_2}]	[σ e^- donation 3p{**2**}→ 5d of Dy {DyX_2}]	[σ e^- donation 3p{**2**} → 5d of Dy{DyX_2}]

Table S6 shows the shape ETS-NOCV computed for the first three highest electron deformation densities, $\Delta Eorb_{(1)-(3)}$. In each figure, orbital interaction (ΔE_{orb}) strength and eigenvalue υ_i are given, giving quantitative information of the amount of displaced charge. The direction of the charge flow of the deformation densities is from red to blue, representing the ring's 2p/3p orbital of O/S of the donor, while the 5d/6s orbital of Dy {DyX_2} fragment is the acceptor. The contours of electron deformation densities confirm the presence of σ-interaction between the p-orbital of the rings and 5d/6s orbitals of the Dy. In the $\mathbf{1_X}$ series, we observe that the $\Delta Eorb_{(1)}$ and the $\Delta Eorb_{(2)}$ arise due to the donation of the electron from the 2p orbital of the O atom to 5d of Dy, whereas $\Delta Eorb_{(3)}$ emerges from the 2p orbital of the O atom to 6s-orbital of Dy. In the $\mathbf{2_X}$ family of complexes, we observed that the most substantial interaction ($\Delta Eorb_{(1)}$) arises from the 3p orbital of the S to 6s-orbital of Dy, suggesting stronger 3p-6s overlap than the 3p-5d overlap. Moreover, the computed $\Delta Eorb_{(1)}$ magnitude in the $\mathbf{2_X}$ family of complexes is nearly two times higher than what we observed in 1X complexes, suggesting enhanced overlap due to the 3p orbital of the S atom. In addition, we observe that the magnitude of the υ_i increases marginally from -F to -I analogue in both the series, which indicates that the amount of electron density flow from ring to Dy increases as we move lighter halides to heavier halides.

Table S8: NBO computed Natural Population Analysis and the NPA Charges of the Dy and O/S centres of complexes $\mathbf{1_X}$-$\mathbf{2_X}$.

	Dy		O/S	
	NPA	**NPA Charge**	**NPA**	**Avg. NPA Charges**
$\mathbf{1_F}$	[core]6s(0.05)4f(2.05)5d(0.30)	2.121	[core]2s(0.98)2p(2.88)	-0.751
$\mathbf{1_{Cl}}$	[core]6s(0.09)4f(2.03)5d(0.43)	1.833	[core]3s(0.96)3p(2.84)	-0.722
$\mathbf{1_{Br}}$	[core]6s(0.10)4f(2.03)5d(0.46)	1.825	[core]4s(0.96)4p(2.81)	-0.750
$\mathbf{1_I}$	[core]6s(0.13)4f(2.04)5d(0.52)	1.287	[core]5s(0.95)5p(2.77)	-0.510
$\mathbf{2_F}$	[core]6s(0.11)4f(2.07)5d(0.37)	1.846	[core]3s(0.80)3p(2.04)	0.211
$\mathbf{2_{Cl}}$	[core]6s(0.16)4f(2.03)5d(0.57)	1.378	[core]3s(0.96)3p(2.84)	0.232
$\mathbf{2_{Br}}$	[core]6s(0.18)4f(2.02)5d(0.62)	1.293	[core]3s(0.80)3p(2.02)	0.236
$\mathbf{2_I}$	[core]6s(0.21)4f(2.02)5d(0.72)	0.569	[core]3s(0.79)3p(2.03)	0.249

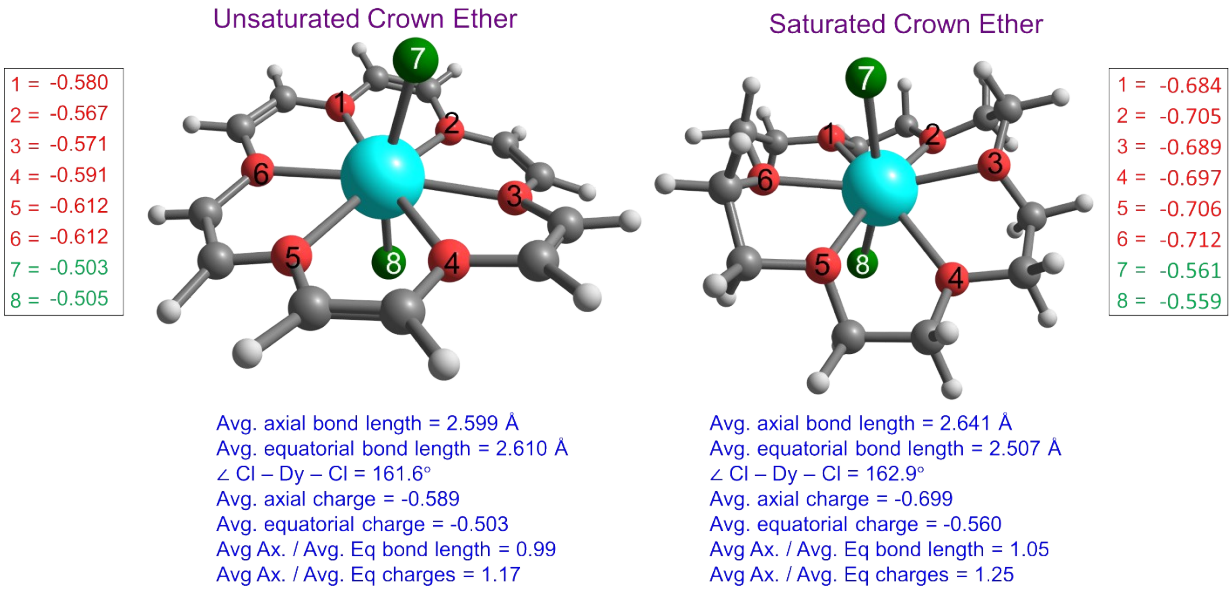

Figure S3: Selected bond parameters and CASSCF computed Mulliken Charges (inset) on the first coordination sphere atoms for $[Dy(U18C6)Cl_2]^+$ (left) and $[Dy(18C6)Cl_2]^+$ (right) along with select bond parameters. Color code Cyan (Dy), Red (O), Dark green (Cl), Grey (C), White (H).

SUPPORTING INFORMATION

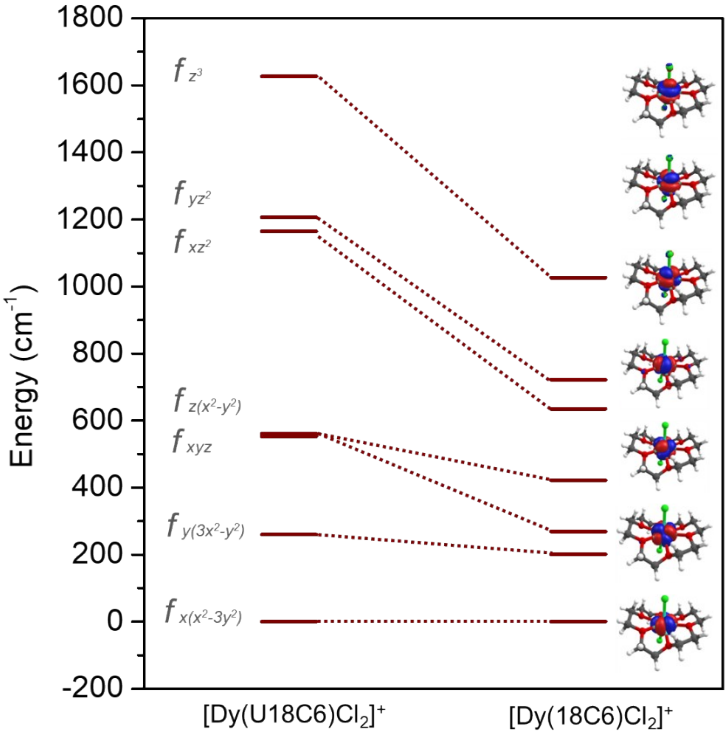

Figure S4: AILFT computed splitting pattern of 4*f* orbitals in the complex $[Dy(18C6)Cl_2]^+$ and $[Dy(U18C6)Cl_2]^+$ series.

Table S9: CASSCF-SO computed electronic states along with the corresponding g-tensor values for $[Dy(18C6)Cl_2]^+$ (saturated $\mathbf{1_{Cl}}$), $[Dy(U18C6)Cl_2]^+$ ($\mathbf{1_{Cl}}$), saturated $\mathbf{2_{Cl}}$ and $\mathbf{2_{Cl}}$. All the energies are reported in cm^{-1}.

	Saturated 1_{Cl}					1_{Cl}				
	Spin-free states	**SOC states ($^6H_{15/2}$)**	**g-values** $g_{xx}; g_{yy}; g_{zz}$			**Spin-free states**	**SOC states ($^6H_{15/2}$)**	**g-values** $g_{xx}; g_{yy}; g_{zz}$		
	0.0					0.0				
	6.0					0.3				
	392.4	0.00	0.0066	0.0085	19.8726	660.5	0.0	0.0000	0.0000	19.9887
	424.2	269.48	0.2849	0.3482	16.9097	669.5	381.3	0.0363	0.0363	17.0730
	537.3	460.43	0.9498	1.9048	12.7672	1002.7	704.2	0.0000	0.0109	14.2109
	593.3	535.12	2.4262	5.8277	12.5307	1093.4	929.6	0.0415	0.0462	10.9288
^6H	604.3	583.18	0.8166	3.2658	12.5678	1134.8	1036.3	8.9575	8.9042	4.6530
	646.9	622.61	0.7999	4.0404	12.9150	1141.5	1097.5	11.4708	9.7305	1.2547
	757.0	680.91	3.2864	4.3477	8.7708	1196.1	1112.7	0.2804	1.4529	3.2461
	800.0	740.03	0.9945	3.1542	16.1956	1216.5	1132.5	9.4810	8.3278	2.1069
	862.7					1233.6				
	7655.6					7967.3				
	7776.3					8100.2				
	7784.9					8113.9				
^6F	7811.1					8244.7				
	7923.1					8330.8				
	7958.2					8332.5				
	7968.3					8349.3				
^6P	34187.1					34130.2				
	34802.0					35421.5				

	34915.0					35439.6				

	Saturated 2_{Cl}					2_{Cl}				
	Spin-free states	**SOC states ($^6H_{15/2}$)**	**g-values** $g_{xx}; g_{yy}; g_{zz}$			**Spin-free states**	**SOC states ($^6H_{15/2}$)**	**g-values** $g_{xx}; g_{yy}; g_{zz}$		
^{6}H	0.0	0.0				0.0				
	1.8	669.9				0.3				
	283.4	1270.1	0.0066	0.0085	19.8726	660.5	0.0	0.0000	0.0000	19.9887
	299.7	1725.2	0.2849	0.3482	16.9097	669.5	381.3	0.0363	0.0363	17.0730
	429.7	1972.2	0.9498	1.9048	12.7672	1002.7	704.2	0.0000	0.0109	14.2109
	447.1	2031.0	2.4262	5.8277	12.5307	1093.4	929.6	0.0415	0.0462	10.9288
	473.1	2062.8	0.8166	3.2658	12.5678	1134.8	1036.3	8.9575	8.9042	4.6530
	593.3	2094.7	0.7999	4.0404	12.9150	1141.5	1097.5	11.4708	9.7305	1.2547
	627.9		3.2864	4.3477	8.7708	1196.1	1112.7	0.2804	1.4529	3.2461
	706.7		0.9945	3.1542	16.1956	1216.5	1132.5	9.4810	8.3278	2.1069
	714.4					1233.6				
^{6}F	7620.9					7967.3				
	7629.1					8100.2				
	7640.3					8113.9				
	7704.2					8244.7				
	7783.1					8330.8				
	7804.1					8332.5				
	7840.9					8349.3				
^{6}P	34007.5					34130.2				
	34590.4					35421.5				
	34715.1					35439.6				

SUPPORTING INFORMATION

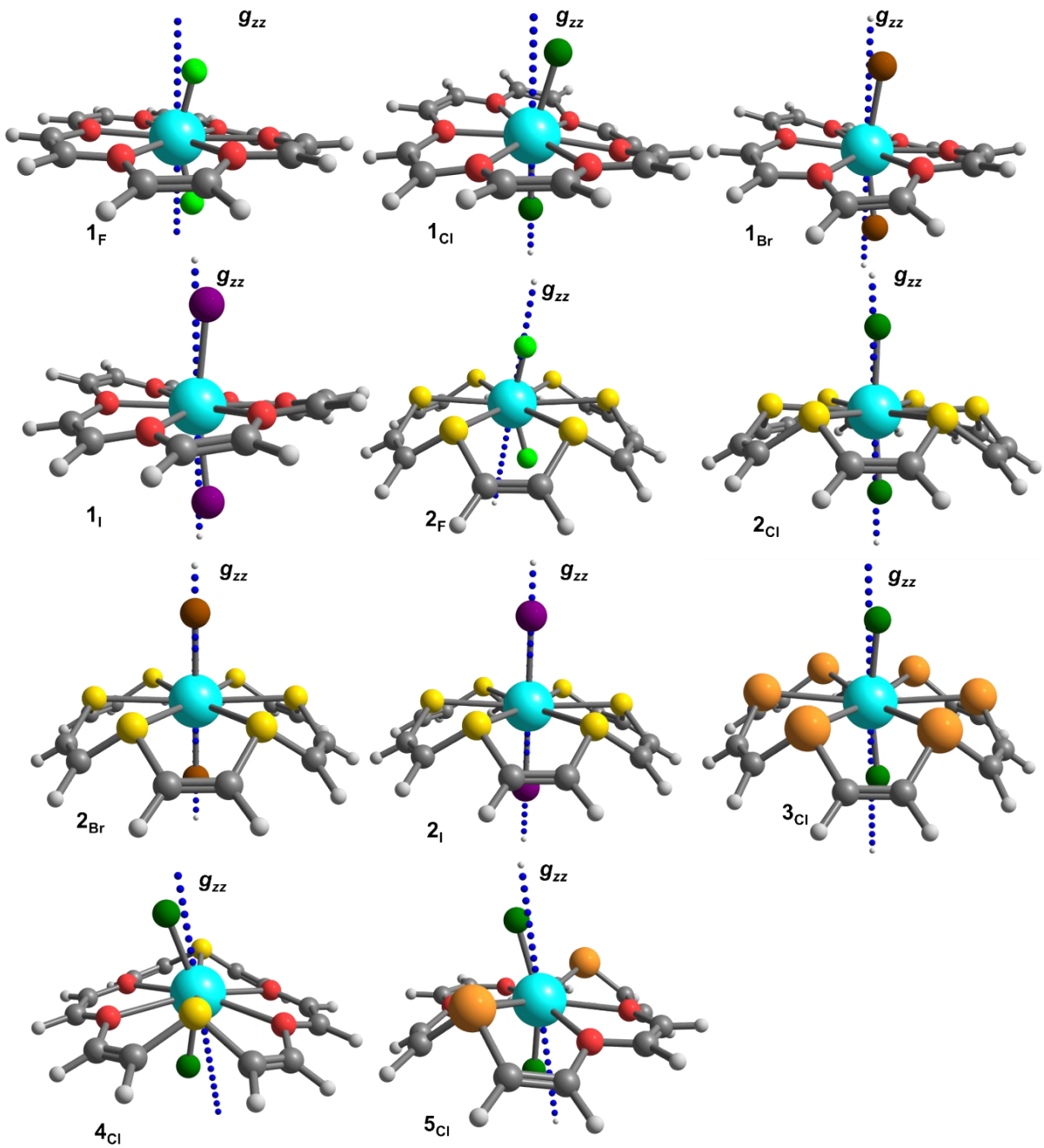

Figure S5: CASSCF computed main magnetic axis (g_{zz}) in complexes $\mathbf{1_X}$-$\mathbf{5_X}$. The dotted blue lines denotes orientation of the main magnetic anisotropy axis (g_{zz}). Color code Cyan (Dy), Red (O), Yellow (S), Orange (Se), Light Green (F), Dark green (Cl), Brown (Br), Violet(I), Grey (C), White (H).

SUPPORTING INFORMATION

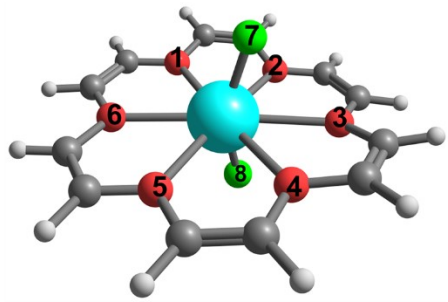

1 = -0.625
2 = -0.595
3 = -0.598
4 = -0.632
5 = -0.643
6 = -0.643
7 = -0.691
8 = -0.693

1_F

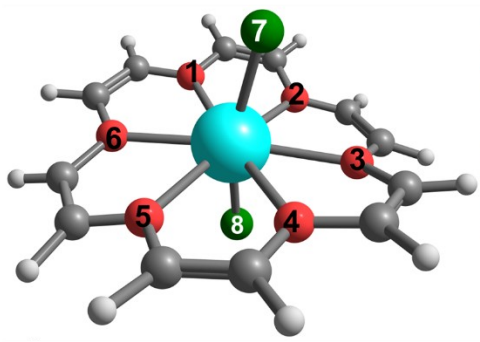

1 = -0.580
2 = -0.567
3 = -0.571
4 = -0.591
5 = -0.612
6 = -0.612
7 = -0.503
8 = -0.505

1_{Cl}

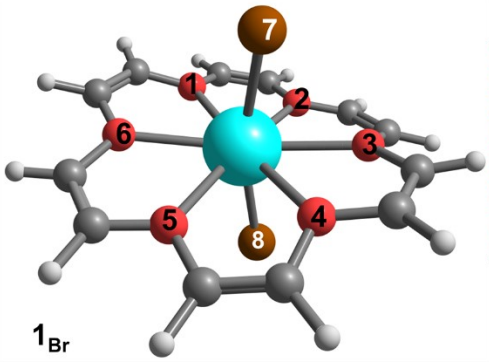

1 = -0.579
2 = -0.566
3 = -0.571
4 = -0.590
5 = -0.610
6 = -0.609
7 = -0.515
8 = -0.514

1_{Br}

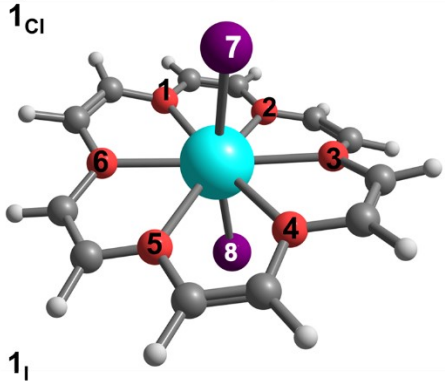

1 = -0.591
2 = -0.582
3 = -0.580
4 = -0.588
5 = -0.607
6 = -0.613
7 = -0.473
8 = -0.470

1_I

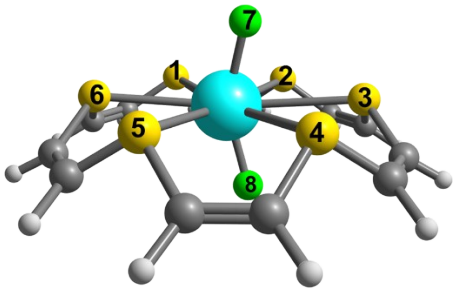

1 = -0.182
2 = -0.180
3 = -0.175
4 = -0.180
5 = -0.176
6 = -0.179
7 = -0.674
8 = -0.689

2_F

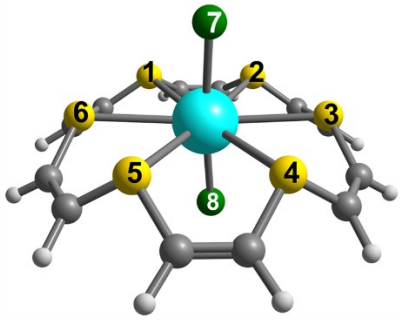

1 = -0.176
2 = -0.175
3 = -0.173
4 = -0.171
5 = -0.174
6 = -0.172
7 = -0.479
8 = -0.513

2_{Cl}

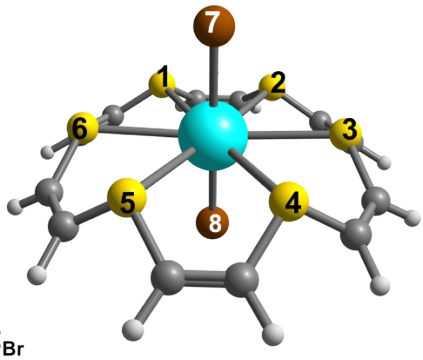

1 = -0.170
2 = -0.169
3 = -0.170
4 = -0.170
5 = -0.169
6 = -0.169
7 = -0.484
8 = -0.522

2_{Br}

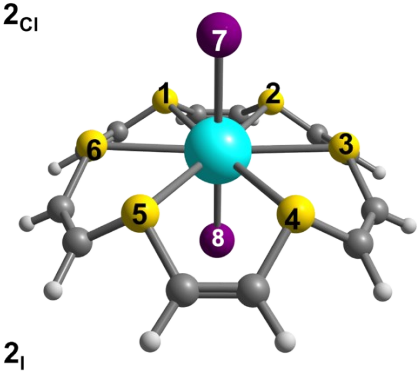

1 = -0.169
2 = -0.166
3 = -0.167
4 = -0.168
5 = -0.169
6 = -0.167
7 = -0.412
8 = -0.453

2_I

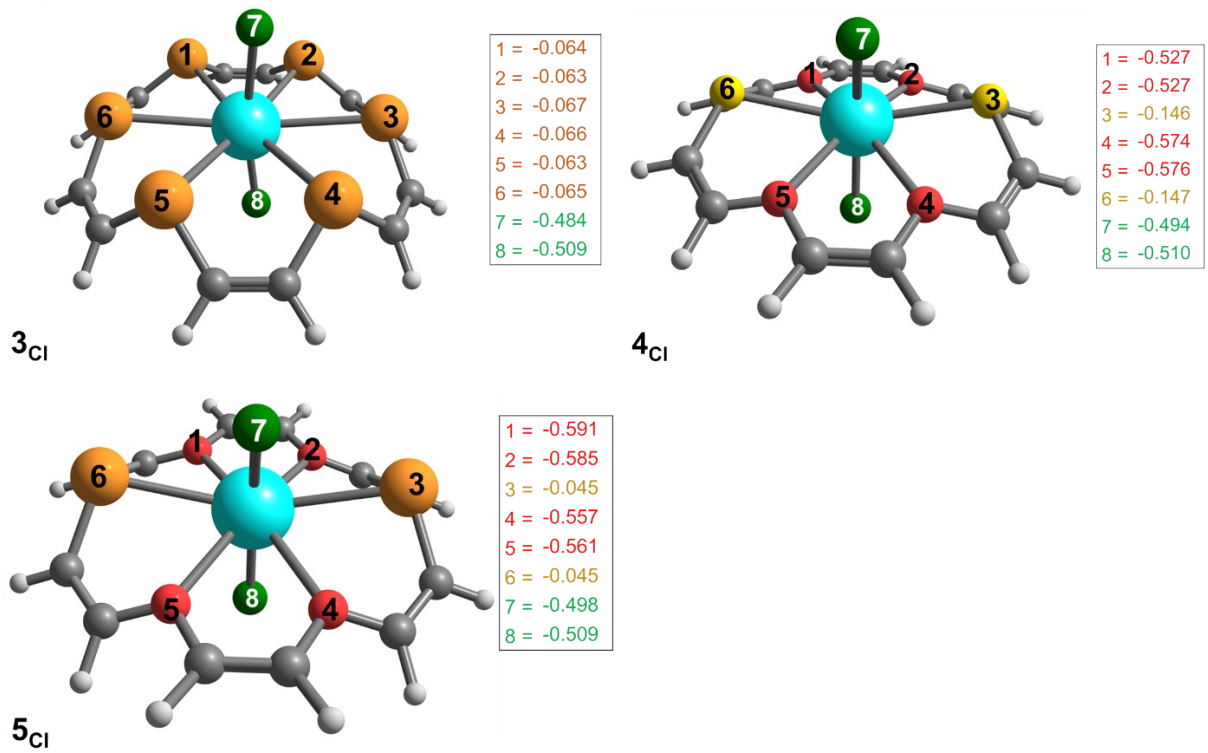

Figure S6: CASSCF computed Mulliken Charges for the atoms in the first coordination sphere for complexes $\mathbf{1_X}$-$\mathbf{5_X}$. Color code Cyan (Dy), Red (O), Yellow (S), Orange (Se), Light Green (F), Dark green (Cl), Brown (Br), Violet(I), Grey (C), White (H).

Ab initio ligand field theory (AILFT) analysis

To investigate the bonding and covalent characteristics within these complexes, we have analysed the interelectronic repulsion parameters (E^1, E^2, and E^3) and the SOC (ζ) parameters for both the free ions and $\mathbf{1_X}$-$\mathbf{5_X}$ complexes using AILFT. The calculated interelectronic repulsion values and their corresponding Racah parameters can be found in Tables S10 to S11. In CASSCF calculations, the computed E^1, E^2, and E^3 parameters for free Dy(III) ions are as follows: 7682.6, 42.6, and 817.2 cm^{-1}. The computed E^1, E^2, and E^3 parameters for the complexes are observed to be lower than those of the free ions. This phenomenon reflects the nephelauxetic effect, resulting from a combination of covalent effects and the dispersion of the metal charge by the ligands. Owing to the inherently confined spatial distribution of the 4*f*-orbital radial wavefunctions, the participation of the 4*f*-electrons in bonding is notably restricted compared to the availability of vacant 5d, 6s, and 6p orbitals. Across all the examined complexes, a consistent reduction of approximately 0.5% to 0.7% has been observed in the E^1, E^2, and E^3 parameters. Additionally, we have noted a reduction in the ζ parameter of the

complex relative to the free ion, indicating a decrease in the angular momentum of the 4*f* orbital due to complexation. The decrease in the ζ parameter, known as the relativistic nephelauxetic effect, is linked to the orbital dilution effect, which indicates covalent interactions within the system. The computed trend in the reduction of F^2, F^4, and F^6 and ζ parameters for all the studied complexes is provided in Fig. S5. Moreover, the Mulliken charges calculated using CASSCF consistently show a greater charge transfer from ligands to the Dy(III) 5*d* orbitals compared to the 4*f* orbitals, primarily attributed to the more diffuse characteristics of the 5*d* orbitals. An examination of Mulliken charge transfer analysis consistently reveals a population of 4*f* orbitals in the studied complexes, ranging from 0.14 to 0.30 electrons, underscoring the evident presence of small 4*f* covalency within these investigated complexes (refer to Fig S9 for details).

To investigate differences in bonding nature and covalency between $[Dy(U18C6)Cl_2]^+$ and $[Dy(18C6)Cl_2]^+$, we have analyzed the splitting pattern of f-orbitals in both complexes. A notable splitting of ~ 1629 cm^{-1} was observed for the former, whereas only ~1026 cm^{-1} for the latter, which is only ~ 63% of the value of $[Dy(U18C6)Cl_2]^+$. In both the cases, we have observed a distinct orbital order, with the sequence of $f_{z3} > f_{yz2} > f_{xz2} > f_{z(x2-y2)}/f_{xyz} > f_{y(3x2-y2)} > f_{x(x2-3y2)}$, which arises from the σ-type interactions between the $3p_z$ ligand (Cl^-) orbitals of the ring and the 4*f* orbitals of Dy(III) ions. The modest *f*-orbital splitting observed in the $[Dy(18C6)Cl_2]^+$ complex indicates a comparatively weak interaction between the 4*f* orbitals and the ligands than $[Dy(U18C6)Cl_2]^+$. In the case of complexes $\mathbf{1_X}$–$\mathbf{2_X}$, a substantial splitting of *f*-orbitals has been observed, spanning a range from 1035 to 2906 cm^{-1}, with the most pronounced splitting being observed in complex $\mathbf{2_F}$. The substantial bond distance between the halide anion (I^-) reduces interaction between the $5p_z$ orbital of the halide and the 4*f* orbital of Dy(III), resulting in the weak splitting for iodide analogue. In summary, the ligand field parameters calculated using AILFT, including the percentage reduction in F^2, F^4, F^6 and ζ values, offer an accurate way to understand the characteristics and intensity of the ligand field within the investigated complexes.

SUPPORTING INFORMATION

Table S10: AILFT computed the Slater Condon parameters F^2, F^4, and F^6, the one-electron effective parameters for spin-orbit coupling (ζ) for complexes $\mathbf{1_X}$-$\mathbf{5_X}$ along with their % reduction at the CASSCF level of theory. All the values provided here are in the cm^{-1}.

Complexes	F^2	F^4	F^6	ζ	F^2(%)	F^4(%)	F^6(%)	ζ(%)
Dy(III) Free Ion	121962.8	76517.7	55041.9	1742.1	-	-	-	-
$\mathbf{1_F}$	121227.8	75931.2	54676.8	1736.1	0.6	0.8	0.7	0.3
$\mathbf{1_{Cl}}$	121245.5	75993.2	54680.2	1735.2	0.6	0.7	0.7	0.4
$\mathbf{1_{Br}}$	121271.0	76022.1	54695.6	1735.0	0.6	0.6	0.6	0.4
$\mathbf{1_I}$	121289.4	76047.2	54705.4	1734.6	0.6	0.6	0.6	0.4
$\mathbf{2_F}$	121167.0	75883.1	54645.3	1735.7	0.7	0.8	0.7	0.4
$\mathbf{2_{Cl}}$	121213.9	75965.0	54664.2	1735.0	0.6	0.7	0.7	0.4
$\mathbf{2_{Br}}$	121221.9	75983.9	54670.1	1734.6	0.6	0.7	0.7	0.4
$\mathbf{2_I}$	121224.0	75999.3	54673.5	1734.1	0.6	0.7	0.7	0.5
$\mathbf{3_{Cl}}$	121229.3	75974.5	54671.3	1735.1	0.6	0.7	0.7	0.4
$\mathbf{4_{Cl}}$	121238.4	75997.8	54681.3	1735.3	0.6	0.7	0.7	0.4
$\mathbf{5_{Cl}}$	121204.2	75965.0	54662.7	1735.0	0.6	0.7	0.7	0.4

Reduction (%) = [1- (complex/free-ion)] * 100

Table S11: AILFT computed the Racah parameters E^1, E^2, and E^3 for complexes $\mathbf{1_X}$-$\mathbf{5_X}$ along with their % reduction at the CASSCF level of theory. All the values provided here are in the cm^{-1}.

Complexes	E^1	E^2	E^3	E^1(%)	E^2(%)	E^3(%)
Dy(III) Free Ion	7632.4	42.4	812.1	-	-	-
$\mathbf{1_F}$	7634.5	42.4	812.4	0.7	0.5	0.6
$\mathbf{1_{Cl}}$	7636.6	42.4	812.6	0.6	0.5	0.6
$\mathbf{1_{Br}}$	7638.1	42.4	812.7	0.6	0.5	0.6
$\mathbf{1_I}$	7628.2	42.4	811.7	0.6	0.5	0.5
$\mathbf{2_F}$	7632.3	42.4	812.2	0.7	0.6	0.7
$\mathbf{2_{Cl}}$	7633.2	42.4	812.2	0.7	0.6	0.6
$\mathbf{2_{Br}}$	7633.7	42.4	812.3	0.6	0.6	0.6
$\mathbf{2_I}$	7633.3	42.4	812.3	0.6	0.6	0.6
$\mathbf{3_{Cl}}$	7634.4	42.4	812.3	0.6	0.6	0.6
$\mathbf{4_{Cl}}$	7631.9	42.4	812.1	0.6	0.6	0.6
$\mathbf{5_{Cl}}$	7682.6	42.6	817.2	0.7	0.6	0.6

Reduction (%) = [1- (complex/free-ion)] * 100

The Racah parameters E^1, E^2 and E^3 (for f-electrons), can be stated in terms of the Slater-Condon parameters F^2, F^4, and F^6, using the following equation:

$$F_2 = \frac{F^2}{225} \quad \text{.....(1)}$$

$$F_4 = \frac{F^4}{1089} \quad \text{..... (2)}$$

$$F_6 = \frac{F^6}{7361.64} \quad \text{..... (3)}$$

$$E^1 = \frac{70F_2 + 231F_4 + 2002F_6}{9} \quad \text{..... (4)}$$

SUPPORTING INFORMATION

$$E^2 = \frac{F_2 - 3F_4 + 7F_6}{9} \quad \ldots\ldots\ldots\ldots\ldots\ldots\ldots\ldots\ldots\ldots\ldots\ldots (5)$$

$$E^3 = \frac{5F_2 + 6F_4 + 91F_6}{3} \quad \ldots\ldots\ldots\ldots\ldots\ldots\ldots\ldots\ldots\ldots\ldots\ldots (6)$$

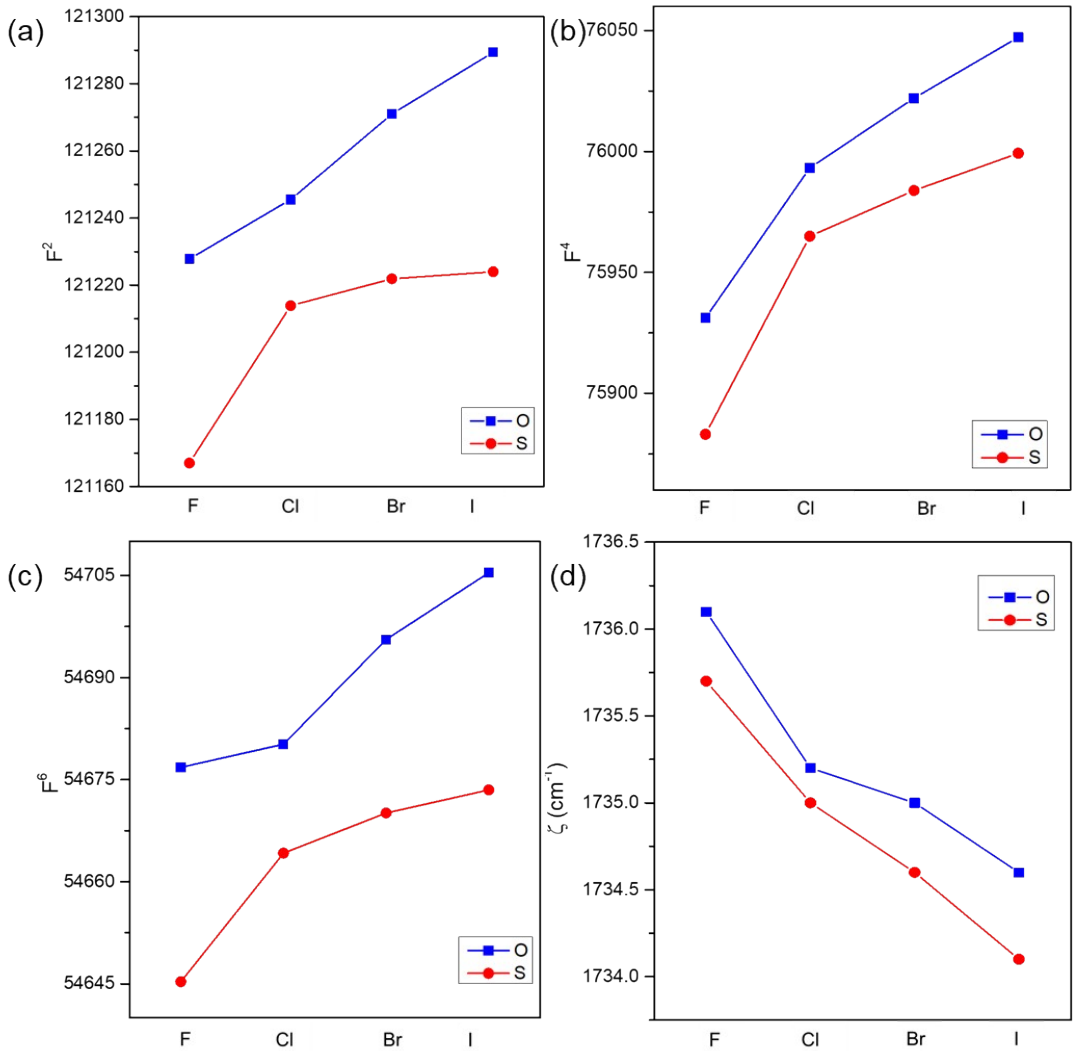

Figure S7: AILFT-CASSCF computed trends in in Slater Condon parameters (a) F^2, (b) F^4 (c) F^6 and (d) ζ for complexes $\mathbf{1_X}$-$\mathbf{2_X}$ series.

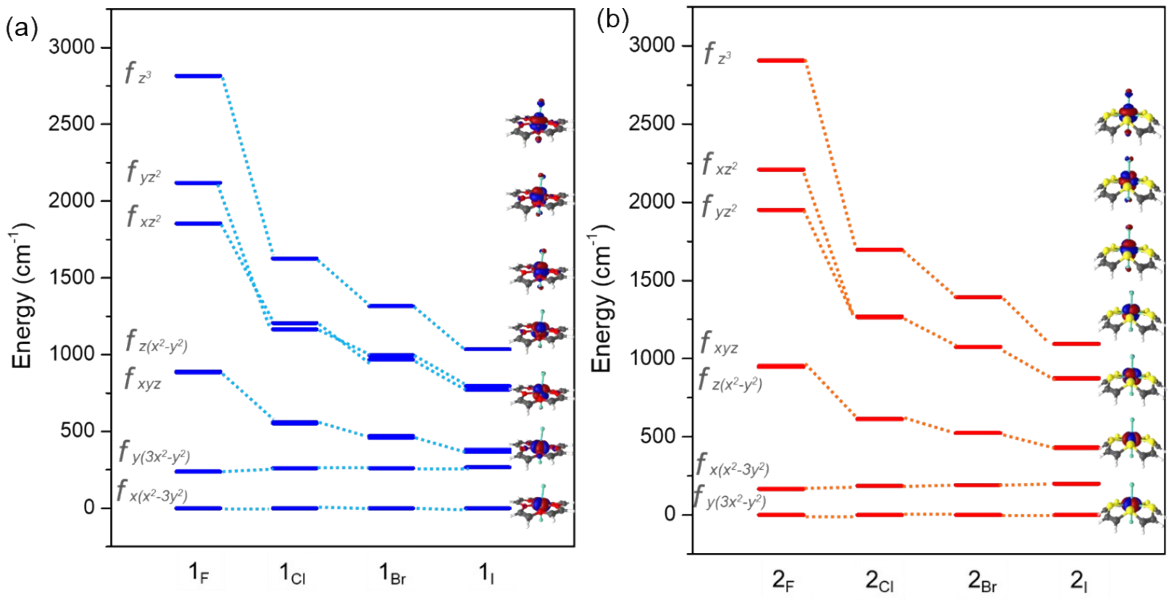

Figure S8: AILFT computed splitting pattern of 4*f* orbitals in the complex $\mathbf{1_X}$ and $\mathbf{2_X}$ series.

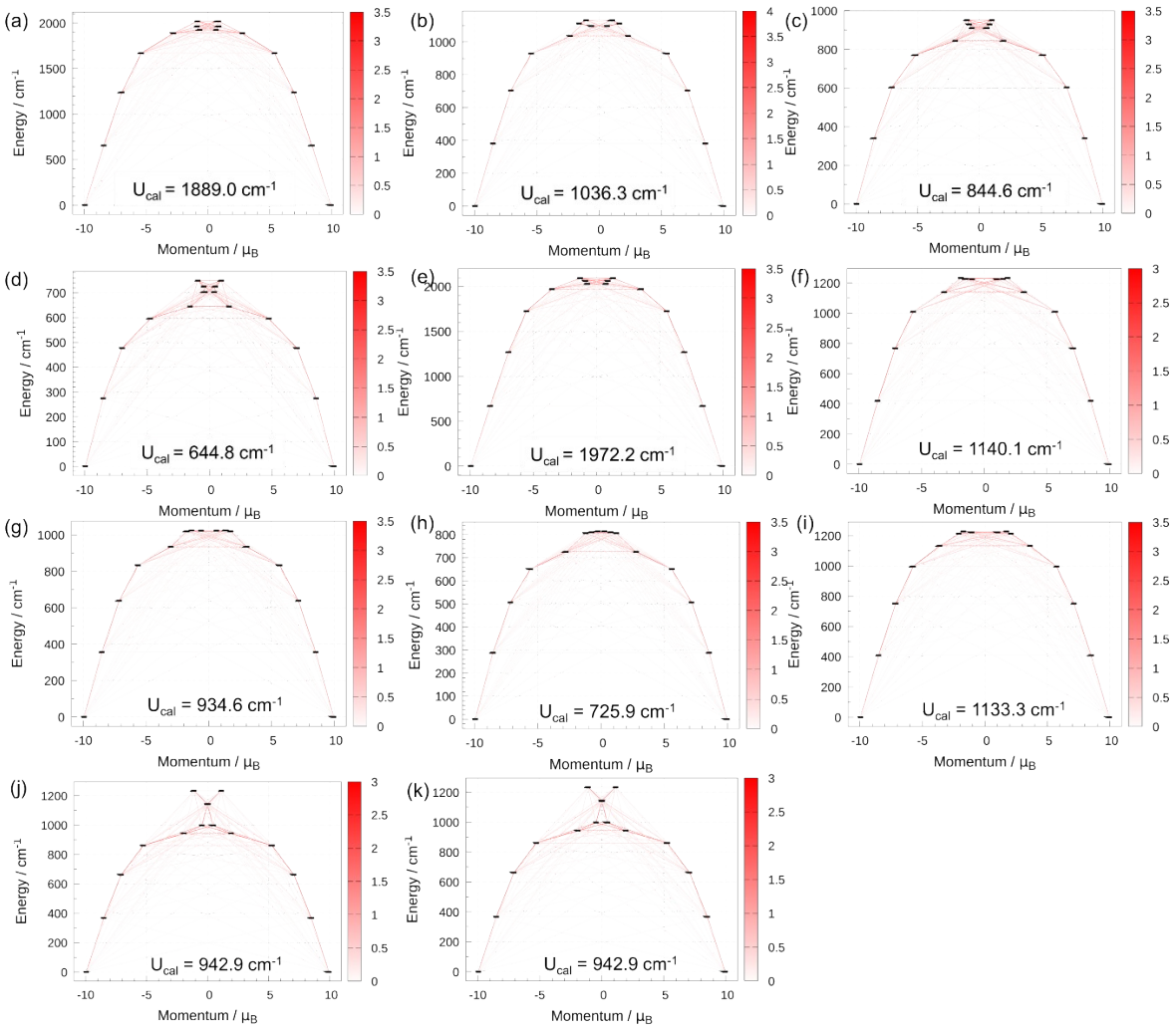

Figure S9: SINGLE_ANISO computed blockade barrier for the complexes (a) $\mathbf{1_F}$ (b) $\mathbf{1_{Cl}}$ (c) $\mathbf{1_{Br}}$ (d) $\mathbf{1_I}$ (e) $\mathbf{2_F}$ (f) $\mathbf{2_{Cl}}$ (g) $\mathbf{2_{Br}}$ (h) $\mathbf{2_I}$ (i) $\mathbf{3_{Cl}}$ (j) $\mathbf{4_{Cl}}$ (k) $\mathbf{5_{Cl}}$ The bold black lines denote the states which are placed according to the values of their magnetic moments. The horizontal lines denote the tunnelling transitions within each doublet state, and the non-horizontal lines correspond to the spin-phonon transition paths. [19] The color intensity of the lines correlates to the amplitude of the averaged transition moments connecting the corresponding states.

Table S12. Calculated U_{eff} (in cm^{-1}) as well as the theoretically predicted three most important excited KDs

Complexes	U_{cal}(cm^{-1})	U_{eff}(cm^{-1})	% contribution from KDs
$\mathbf{1_F}$	1889.0	1710.0	KD1 23% + KD5 18% + KD2 14%
$\mathbf{1_{Cl}}$	1036.3	1087.0	KD5 37% + KD6 33% + KD8 23%
$\mathbf{1_{Br}}$	844.6	890.7	KD5 38% + KD6 26% + KD8 18%
$\mathbf{1_I}$	644.8	686.7	KD5 35% + KD6 27% + KD8 13%
$\mathbf{2_F}$	1972.2	1863.0	KD6 24% + KD5 18% + KD8 16%
$\mathbf{2_{Cl}}$	1140.1	1196.0	KD5 42% + KD6 30% + KD7 14%
$\mathbf{2_{Br}}$	934.6	1008.0	KD5 33% + KD7 27% + KD6 22%
$\mathbf{2_I}$	725.9	797.3	KD5 35% + KD7 26% + KD6 26%
$\mathbf{3_{Cl}}$	1133.3	1201.0	KD5 42% + KD6 29% + KD7 22%
$\mathbf{4_{Cl}}$	942.9	960.3	KD5 44% + KD4 18% + KD6 17%
$\mathbf{5_{Cl}}$	1043.0	1039.0	KD5 36% + KD6 28% + KD4 22%

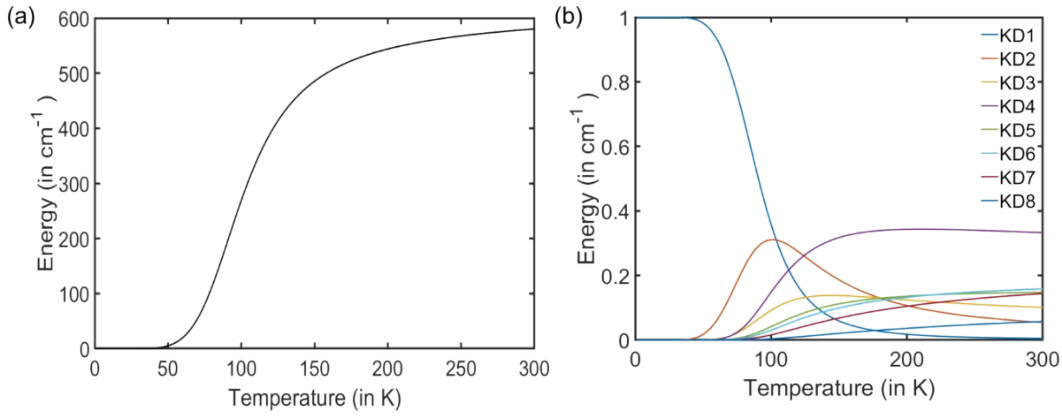

Figure S10: (a) Temperature dependence of calculated U_{eff} for **[Dy(18C6)Cl$_2$]$^+$**, (b) relative contribution of each Kramer's doublet to the relaxation calculated as $k_i(T)/N_k$.

SUPPORTING INFORMATION

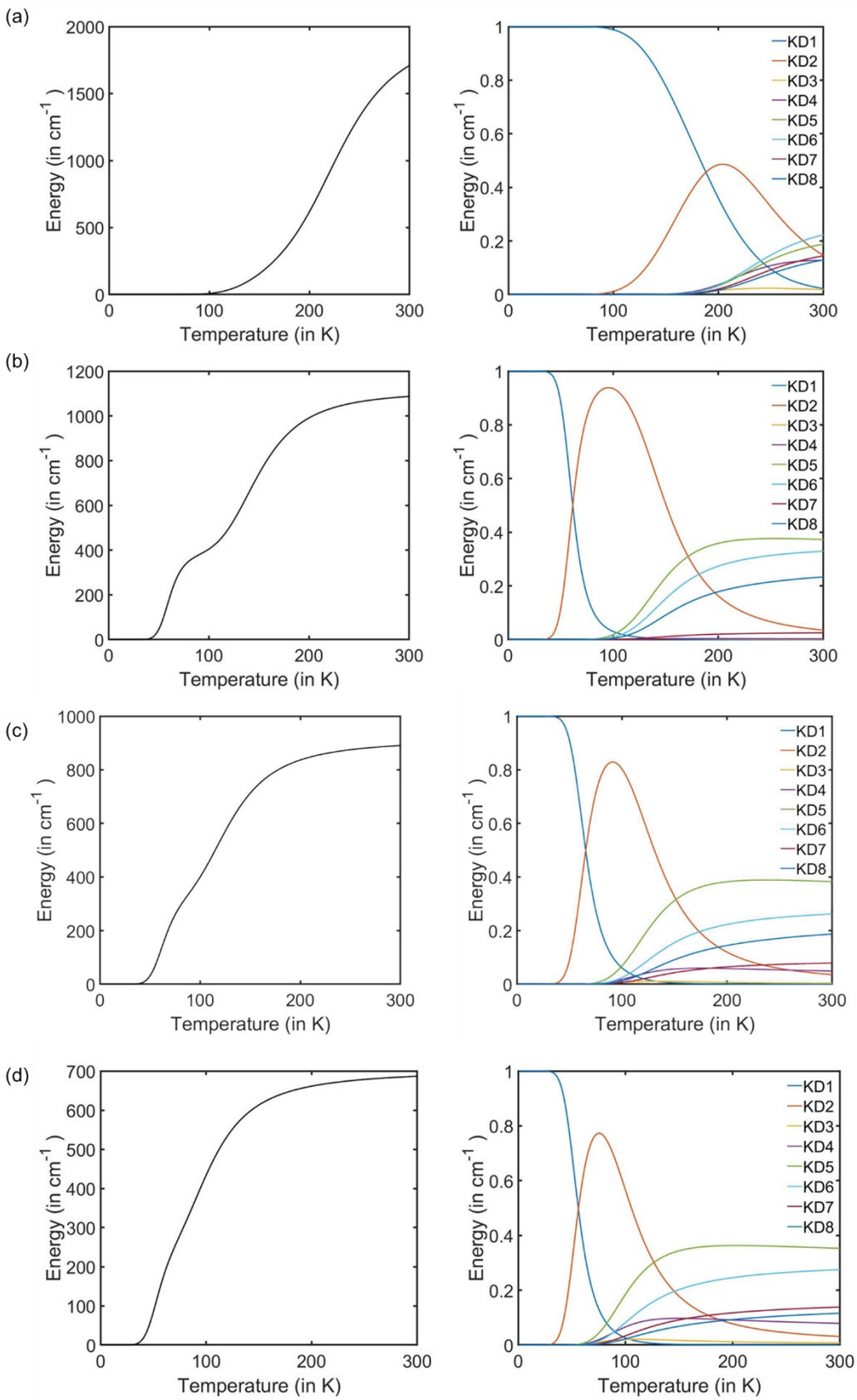

Figure S11: (a)-(d) Temperature dependence of calculated U_{eff} for $\mathbf{1_F}$, $\mathbf{1_{Cl}}$, $\mathbf{1_{Br}}$ and $\mathbf{1_I}$ (right) and relative contribution of each Kramer's doublet to the relaxation calculated as $k_i(T)/N_k$ (left).

SUPPORTING INFORMATION

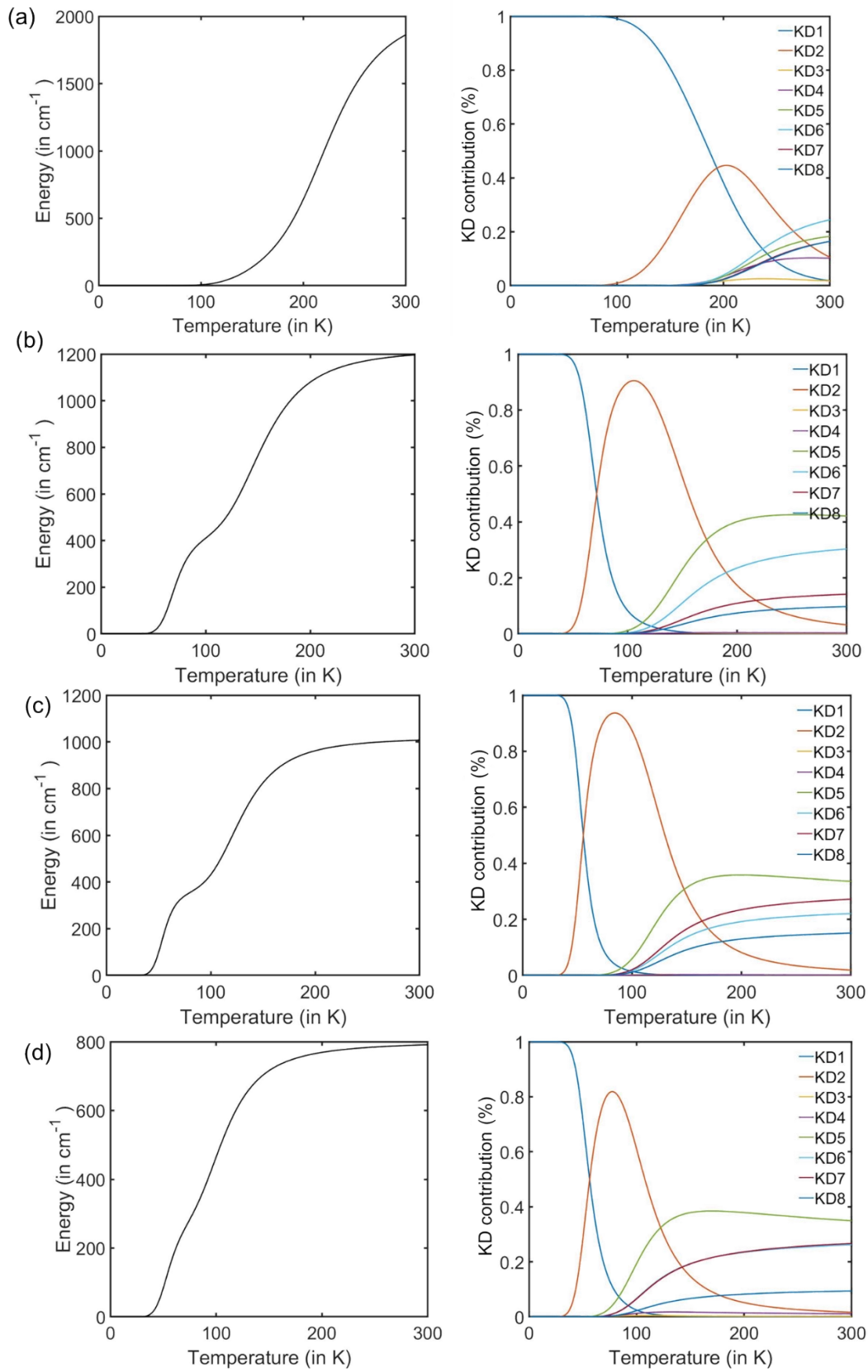

Figure S12: (a)-(d) Temperature dependence of calculated U_{eff} for $\mathbf{2_F}$, $\mathbf{2_{Cl}}$, $\mathbf{2_{Br}}$ and $\mathbf{2_I}$ (right) and relative contribution of each Kramer's doublet to the relaxation calculated as $k_i(T)/N_k$ (left).

SUPPORTING INFORMATION

Magnetic anisotropy calculations in model complexes with bulky axial ligands

In order to synthesise and isolate these complexes, we often require a bulky group on the axial position to prevent multiple coordination and to maintain the axiality. In addition to our studied complexes **1_X-5_X**, we have prepared two model complexes where we chose the bulky ligands -$OSiPh_3$ and -O^tBu as the axial ligands. In literature the -OSiPh3 ligand has been used as an axial ligand with Schiff-based ligands in $[Dy(L_1^{N6})(Ph_3SiO)_2]^+$ (with U_{eff} = 1080K); [20] $[Dy(L_2^{N6}{}_{R/S})(Ph_3SiO)_2]^+$ (with U_{eff} = 1833 K (R); Ueff = 1819 K (S)); [21] $[DyL_3^{N6}{}_{R/S}(Ph_3SiO)_2]^+$ (with U_{eff} = 1454 K (R); U_{eff} = 1457 K (S))[22]; $[Dy(L_4^{N6})(Ph_3SiO)_2]$ (with U_{eff} 1732 K) [23] to name a few. Similarly, the -O^tBu ligand has been used in $[Dy(O^tBu)_2(L_5)_4]^+$ (U_{eff} = 2075 K); [24] $[Dy(O^tBu)_2(py)_5]^+$ (U_{eff}= 1815 K) [25]. Here, we have prepared model complexes of thia crowns, where these bulky ligands occupy the axial positions and complexes are named **2_{OSiPh3}** and **2_{OtBu}**.

(L_1 = Schiff-base ligand derived from 2,6- diacetylpyridine and ethylenediamine; L_2 = Schiff-base ligand derived from 2,6-pyridinedicarboxaldehyde and (1R/S, 2R/S)-1,2-bis(2,4,6-trifluorophenyl)-ethane-1,2-diamine; L_4 =2,5,8- triaza-1 (8,2), 4, 7 (2,8)-triquinolina cyclononaphane -2,5,8-triene; L_5 = 4-phenylpyridine)

For ease of optimisations, we replaced the Dy(III) atom with Lu(III) and carried out optimisations in the same manner as mentioned in the Computational Details. DFT optimized structure shows HBPY-8 geometry (HBPY-8; CShM = 4.753 for **2_{OSiPh3}** and 3.126 for **2_{OtBu}**). For **2_{OSiPh3}** and **2_{OtBu}**, the ratio of the avg. axial to avg. equatorial bond distance is 0.636 and 0.656, showing that the Dy(III) ion stabilizes in the two complexes in an axial ligand field. On these optimized coordinates, we performed CASSCF calculations with an active space of 9 electrons in 7 orbitals i.e., CAS(9,7). The computed SH parameters, along with spin-free and spin-orbit states are provided in Table S19. Our calculations determine an Ising-type anisotropy in the ground state with the g-values g_{zz} ~19.9 and g_{xx}~g_{yy} ~ 1x10^{-3} for both the complexes and the g_{zz} axis for the ground state KD is oriented nearly along the O–Dy–O bond, which coincides with the highest order pseudo C_6 axis. The ground state wavefunction is determined to be m_J $|\pm 15/2\rangle$, further supporting the claim that the dominant axial ligand field is stabilised around the Dy(III) ion. The CASSCF computed barrier height for both these complexes are 1903.3 cm^{-1} for **2_{OSiPh3}** and 2397.2 cm^{-1} for **2_{OtBu}**, respectively. For both complexes, the orientation of the main magnetic axis (g_{zz}) and the magnetic relaxation pathway is depicted in Figure S13. These findings reveal that the relaxation barrier achieved with bulky ligands is on par with the results obtained from our top-performing complexes, **1_F** and **2_F**.

SUPPORTING INFORMATION

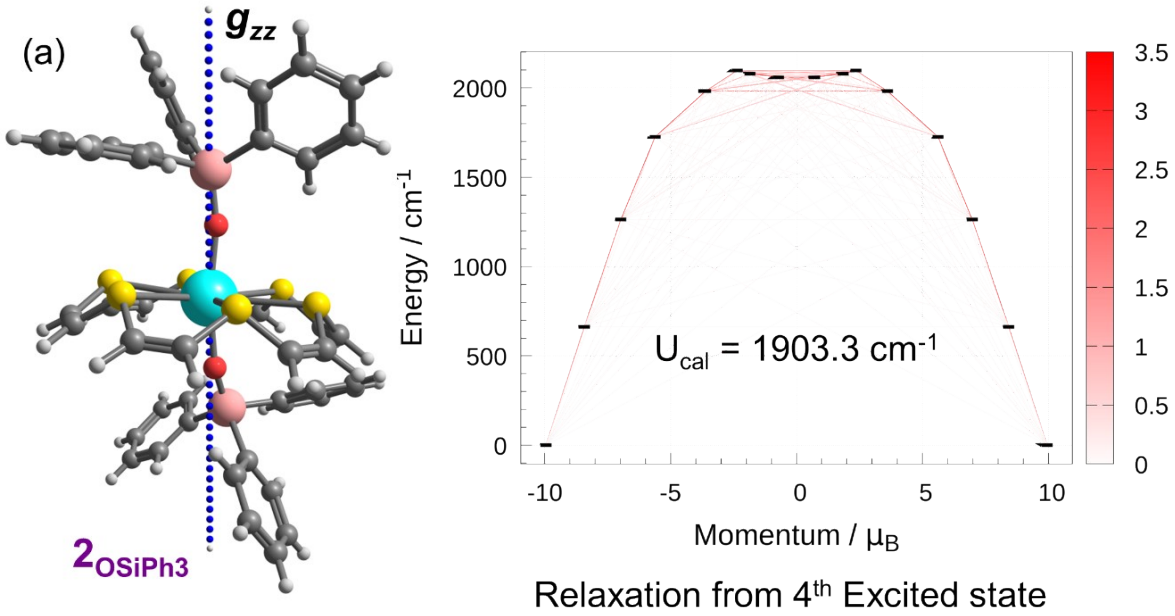

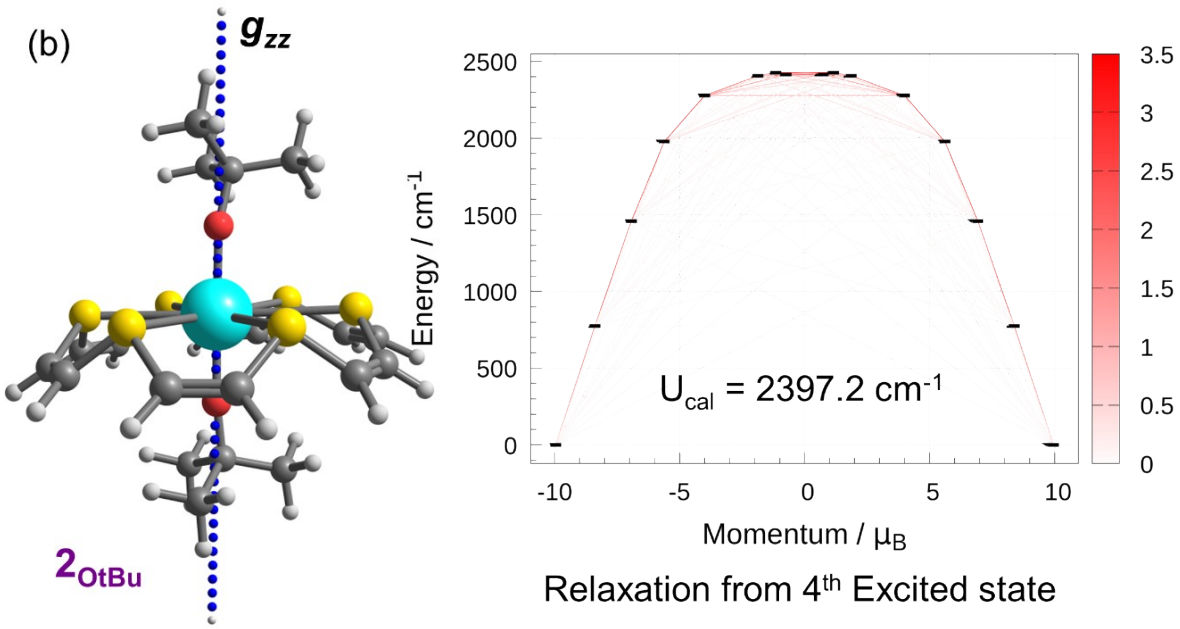

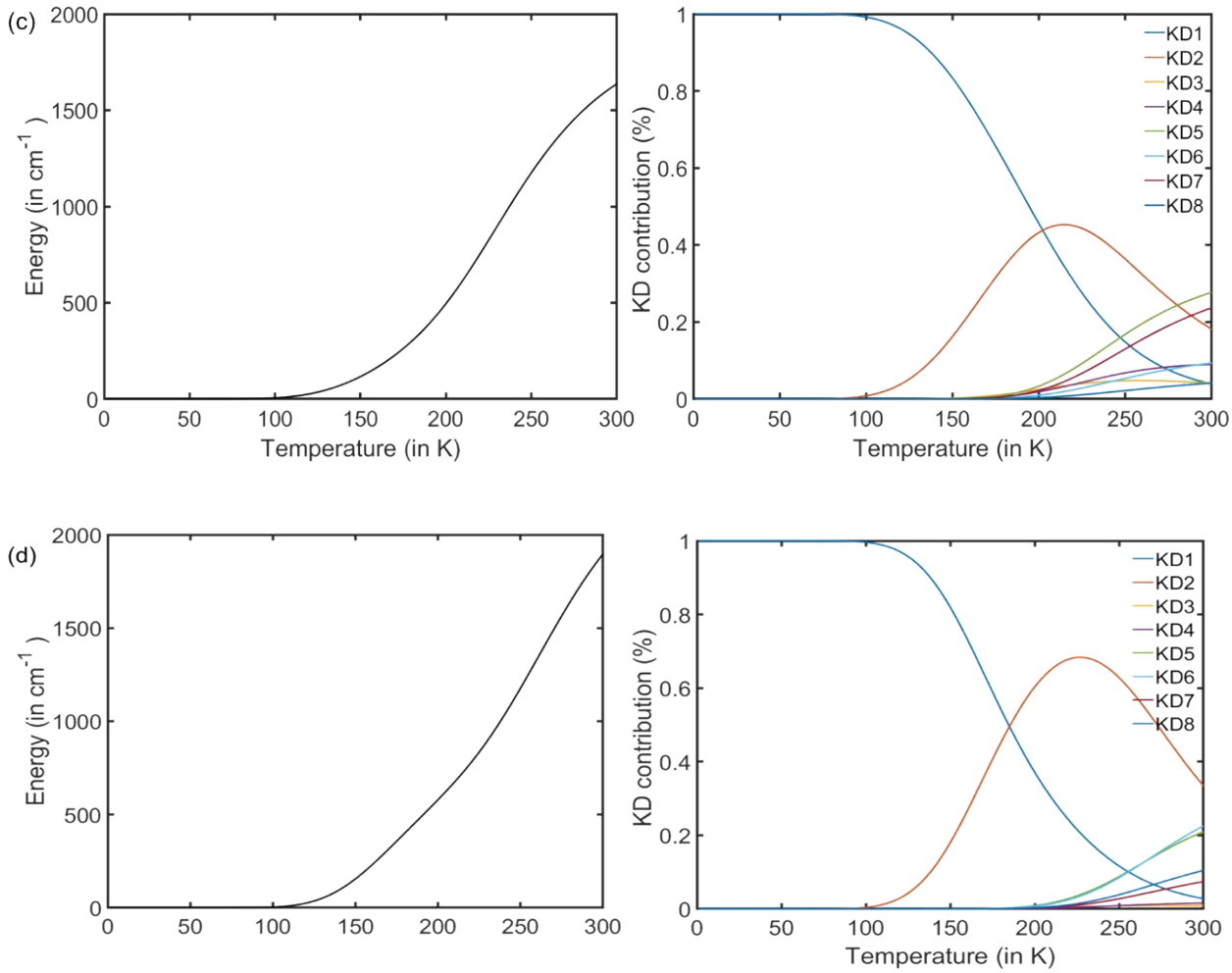

Figure S13: (a) Structure of model complex $\mathbf{2_{OSiPh3}}$ (right) and SINGLE_ANISO computed blockade barrier (left), (b) Structure of model complex $\mathbf{2_{OtBu}}$ (right) and SINGLE_ANISO computed blockade barrier (left). (c) and (d) Temperature dependence of calculated U_{eff} for $\mathbf{2_{OSiPh3}}$, $\mathbf{2_{OtBu}}$ (right) and relative contribution of each Kramer's doublet to the relaxation calculated as $k_i(T)/N_k$ (left). Color code Cyan (Dy), Red (O), Yellow (S), Pink (Si), Grey (C), White (H).

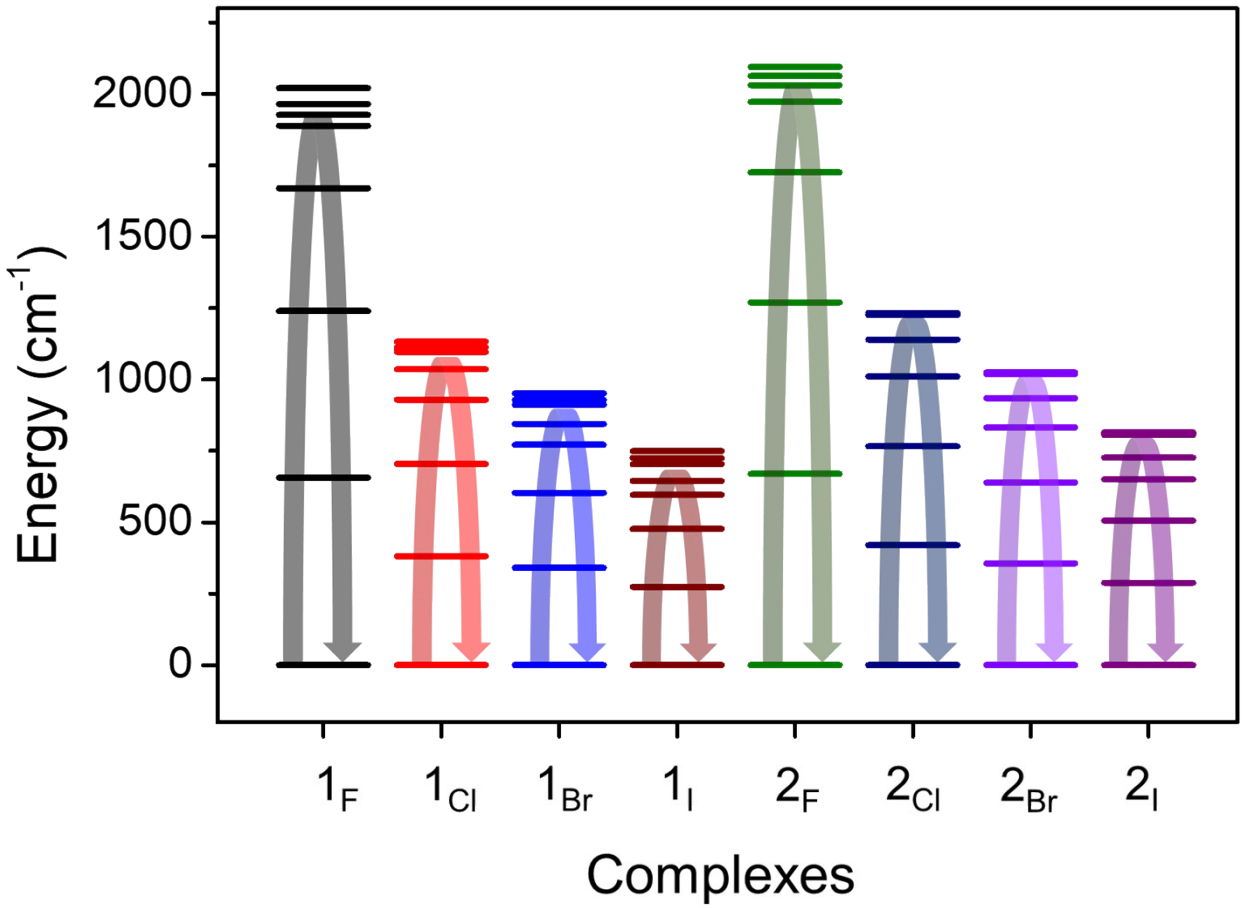

Figure S14. SINGLE_ANISO computed span of the eight KDs for complexes $\mathbf{1_X}$ and $\mathbf{2_X}$. The bold arrows indicate the probable relaxation pathway

Table S13. SINGLE_ANISO computed wave function decomposition analysis for the Dy(III) centre. The major dominating values are kept in bold.

±*mJ*	*wave function decomposition analysis* $\mathbf{1_F}$
KD1	**99.9 % |±15/2〉**
KD2	**99.8 % |±13/2〉**
KD3	**99.1 % |±11/2〉**
KD4	**93.6 % |±9/2〉**
KD5	**69.1 % |±7/2〉** + 15.7% |±5/2〉 + 10.6% |±3/2〉
KD6	**93.7 % |±1/2〉**
KD7	**73.2 % |±3/2〉** + 19.1% |±5/2〉
KD8	**60.5 % |±5/2〉** + 25.3% |±7/2〉
±*mJ*	*wave function decomposition analysis* $\mathbf{1_{Cl}}$
KD1	**99.9 % |±15/2〉**
KD2	**99.8 % |±13/2〉**
KD3	**99.1 % |±11/2〉**
KD4	**95.2 % |±9/2〉**
KD5	**71.4 % |±7/2〉** + 28.5% |±5/2〉
KD6	**93.7 % |±1/2〉**
KD7	**94.8 % |±3/2〉**
KD8	**71.3 % |±5/2〉** + 28.3% |±7/2〉
±*mJ*	*wave function decomposition analysis* $\mathbf{1_{Br}}$
KD1	**99.9 % |±15/2〉**
KD2	**99.8 % |±13/2〉**
KD3	**99.1 % |±11/2〉**
KD4	**88.1 % |±9/2〉** + 8.5% |±3/2〉
KD5	**61.4 % |±7/2〉** + 35.1% |±5/2〉
KD6	**84.9 % |±1/2〉** + 11.3 % |±3/2〉
KD7	**70.7 % |±3/2〉** + 13.6 % |±1/2〉
KD8	**60.9 % |±5/2〉** + 30.7% |±7/2〉
±*mJ*	*wave function decomposition analysis* $\mathbf{1_I}$
KD1	**99.9 % |±15/2〉**
KD2	**99.8 % |±13/2〉**
KD3	**99.1 % |±11/2〉**
KD4	**81.1 % |±9/2〉** + 13.2% |±3/2〉
KD5	**55.6 % |±7/2〉** + 39.0 % |±5/2〉
KD6	**81.2 % |±1/2〉** + 11.5 % |±3/2〉
KD7	**65.6 % |±3/2〉** + 14.8 % |±1/2〉 + 12.1 % |±9/2〉
KD8	**55.3 % |±5/2〉** + 35.0 % |±7/2〉
±*mJ*	*wave function decomposition analysis* $\mathbf{2_F}$
KD1	**99.9 % |±15/2〉**
KD2	**99.8 % |±13/2〉**
KD3	**99.1 % |±11/2〉**
KD4	**96.2 % |±9/2〉**
KD5	**78.5 % |±7/2〉** + 10.5 % |±3/2〉
KD6	**91.5 % |±1/2〉** + 3.8 % |±3/2〉

KD7	**67.6 % |±3/2〉** + 22.1 % |±5/2〉
KD8	**63.3 % |±5/2〉** + 17.6 % |±3/2〉 + 15.7 % |±7/2〉
±mJ	*wave function decomposition analysis* $\mathbf{2_{Cl}}$
KD1	**99.9 % |±15/2〉**
KD2	**99.8 % |±13/2〉**
KD3	**99.6 % |±11/2〉**
KD4	**97.2 % |±9/2〉**
KD5	**82.1 % |±7/2〉** + 17.5 % |±5/2〉
KD6	**68.6 % |±1/2〉** + 20.2 % |±3/2〉
KD7	**44.6 % |±5/2〉** + 27.0 % |±1/2〉 + 17.6 % |±3/2〉 + 10.2 % |±7/2〉
KD8	**60.3 % |±3/2〉** + 29.1 % |±5/2〉
±mJ	*wave function decomposition analysis* $\mathbf{2_{Br}}$
KD1	**99.9 % |±15/2〉**
KD2	**99.8 % |±13/2〉**
KD3	**99.6 % |±11/2〉**
KD4	**97.4 % |±9/2〉**
KD5	**80.3 % |±7/2〉** + 17.5 % |±5/2〉
KD6	**78.6 % |±5/2〉** + 19.2 % |±7/2〉
KD7	**76.6 % |±1/2〉** + 21.7 % |±3/2〉
KD8	**74.2 % |±3/2〉** + 22.3 % |±5/2〉
±mJ	*wave function decomposition analysis* $\mathbf{2_{I}}$
KD1	**99.9 % |±15/2〉**
KD2	**99.9 % |±13/2〉**
KD3	**99.4 % |±11/2〉**
KD4	**96.1 % |±9/2〉**
KD5	**76.8 % |±7/2〉** + 23.1 % |±5/2〉
KD6	**65.7 % |±5/2〉** + 19.6 % |±7/2〉
KD7	**58.8 % |±3/2〉** + 27.7 % |±1/2〉
KD8	**63.9 % |±1/2〉** + 30.3 % |±3/2〉

SUPPORTING INFORMATION

Table S14: CASSCF-SO computed electronic states along with the corresponding g-tensor values for complexes $\mathbf{1_X}$. All the energies are reported in cm^{-1}.

	$\mathbf{1_F}$					$\mathbf{1_{Cl}}$				
	Spin-free states	**SOC states ($^6H_{15/2}$)**	**g-values** g_{xx}; g_{yy}; g_{zz}			**Spin-free states**	**SOC states ($^6H_{15/2}$)**	**g-values** g_{xx}; g_{yy}; g_{zz}		
^{6}H	0.0	0.0	0.0000	0.0000	19.908	0.0	0.0	0.0000	0.0000	19.9887
	0.2	656.6	0.013	0.014	16.852	0.3	381.3	0.0363	0.0363	17.0730
	1136.8	1239.3	0.024	0.033	13.925	660.5	704.2	0.0000	0.0109	14.2109
	1173.0	1669.8	1.49	1.65	10.814	669.5	929.6	0.0415	0.0462	10.9288
	1836.3	1889.0	7.563	6.846	4.7320	1002.7	1036.3	8.9575	8.9042	4.6530
	1855.1	1926.9	1.248	6.726	12.450	1093.4	1097.5	11.4708	9.7305	1.2547
	1899.1	1964.4	1.658	3.321	11.358	1134.8	1112.7	0.2804	1.4529	3.2461
	1990.9	2020.8	0.805	2.642	14.819	1141.5	1132.5	9.4810	8.3278	2.1069
	2085.9					1196.1				
	2121.8					1216.5				
	2150.3					1233.6				
^{6}F	8549.3					7967.3				
	8741.0					8100.2				
	8820.0					8113.9				
	9030.7					8244.7				
	9118.9					8330.8				
	9152.4					8332.5				
	9154.0					8349.3				
^{6}P	34094.1					34130.2				
	36446.2					35421.5				
	36572.4					35439.6				

	1_{Br}					1_I				
	Spin-free states	**SOC states ($^6H_{15/2}$)**	**g-values** g_{xx}; g_{yy}; g_{zz}			**Spin-free states**	**SOC states ($^6H_{15/2}$)**	**g-values** g_{xx}; g_{yy}; g_{zz}		
^{6}H	0.0	0.0	0.0000	0.0001	19.9061	0.0	0.0	0.0001	0.0002	19.9037
	0.4	340.5	0.0753	0.0767	17.0487	1.0	274.3	0.1374	0.1402	17.0642
	539.1	603.7	0.0209	0.0377	14.1676	423.0	476.6	0.0728	0.1068	14.0619
	546.5	771.4	0.8044	0.8337	10.4995	430.3	596.4	1.6088	1.6887	9.7093
	781.8	844.6	9.9871	8.6139	3.7590	583.3	644.8	11.0579	7.9600	2.9970
	893.6	911.1	12.5885	7.9902	0.8969	692.5	703.8	0.6348	4.3812	15.7730
	922.4	928.8	0.5221	1.4315	4.8815	712.5	725.6	0.7425	1.5111	10.2720
	927.1	951.5	11.0494	8.2824	0.3990	723.5	749.5	0.0354	5.3525	13.8691
	972.2					765.5				
	983.6					776.4				
	1003.0					799.5				
^{6}F	7836.6					7713.8				
	7940.3					7795.8				
	7949.6					7802.8				
	8052.7					7872.1				
	8133.3					7954.3				
	8134.6					7958.2				
	8157.3					7978.9				
^{6}P	34145.1					34163.1				
	35168.2					34923.4				
	35179.0					34944.7				

SUPPORTING INFORMATION

Table S15: CASSCF-SO computed electronic states along with the corresponding g-tensor values for complexes $\mathbf{2_X}$. All the energies are reported in cm^{-1}.

	$\mathbf{2_F}$					$\mathbf{2_{Cl}}$				
	Spin-free states	**SOC states ($^6H_{15/2}$)**	**g-values** g_{xx};	g_{yy};	g_{zz}	**Spin-free states**	**SOC states ($^6H_{15/2}$)**	**g-values** g_{xx};	g_{yy};	g_{zz}
^{6}H	0.0	0.0	0.0000	0.0000	19.9125	0.0	0.0	0.0000	0.0000	19.9136
	0.1	669.9	0.0055	0.0059	16.8494	0.0	419.9	0.0180	0.0180	17.0260
	1175.4	1270.1	0.0156	0.0184	13.9389	692.2	766.5	0.0024	0.0027	14.2373
	1198.6	1725.2	0.8372	0.9086	11.1207	692.7	1010.6	0.0310	0.0317	11.3634
	1945.7	1972.2	4.7549	5.0858	7.6711	1079.1	1140.1	7.5278	7.4780	6.3101
	1948.7	2031.0	1.3467	6.5775	12.1897	1207.9	1225.4	11.9517	8.2262	1.2920
	1993.9	2062.8	1.6902	2.5731	11.9714	1211.4	1227.8	1.6505	3.0200	5.5334
	2084.7	2094.7	0.2218	3.4581	14.6005	1239.8	1233.5	0.5055	3.4086	13.1868
	2128.9					1241.3				
	2204.3					1281.9				
	2221.5					1283.3				
^{6}F	8613.7					8019.1				
	8805.4					8152.8				
	8881.8					8154.1				
	9130.5					8342.5				
	9187.8					8380.8				
	9220.4					8381.2				
	9221.8					8407.5				
^{6}P	34048.5					34082.5				
	36552.1					35529.9				
	36677.9					35531.1				

	2_{Br}					2_I				
	Spin-free states	**SOC states ($^6H_{15/2}$)**	**g-values** g_{xx};	g_{yy};	g_{zz}	**Spin-free states**	**SOC states ($^6H_{15/2}$)**	**g-values** g_{xx};	g_{yy};	g_{zz}
^{6}H	0.0	0.0	0.0000	0.0000	19.9129	0.0	0.0	0.0000	0.0000	19.9117
	0.0	356.4	0.0278	0.0278	17.0608	0.1	288.7	0.0484	0.0486	17.0929
	580.0	638.8	0.0010	0.0052	14.2848	462.7	506.4	0.0001	0.0140	14.3109
	580.1	832.3	0.0222	0.0241	11.3214	463.7	650.8	0.1754	0.1901	11.1871
	864.0	934.6	7.8358	7.8218	6.0715	650.7	725.9	8.4398	8.1837	5.5449
	1000.6	1019.7	8.3725	7.3556	3.3424	792.0	806.0	2.3226	3.4460	13.7723
	1018.6	1023.5	0.9274	6.2743	13.9724	816.3	810.8	1.5030	4.9108	13.8273
	1036.9	1024.8	1.3967	4.4024	12.1765	822.5	814.6	0.1219	0.6653	18.4632
	1038.0					824.3				
	1053.5					825.6				
	1053.8					827.3				
^{6}F	7893.4					7766.7				
	7994.9					7838.1				
	7995.1					7839.2				
	8156.0					7966.0				
	8187.6					7996.1				
	8187.9					7996.8				
	8222.0					8034.4				
^{6}P	34093.3					34104.4				
	35275.9					35017.2				
	35277.5					35023.9				

SUPPORTING INFORMATION

Table S16: CASSCF-SO computed electronic states along with the corresponding g-tensor values for complex $\mathbf{3_{Cl}}$. All the energies are reported in cm^{-1}.

	3_{Cl}				
	Spin-free states	**SOC states ($^6H_{15/2}$)**	**g-values** $g_{xx}; g_{yy}; g_{zz}$		
^{6}H	0.0	0.0	0.0000	0.0000	19.9152
	0.0	409.3	0.0110	0.0111	17.0370
	673.5	751.7	0.0019	0.0031	14.2614
	675.2	997.0	0.1073	0.1097	11.4962
	1076.0	1133.3	6.0365	6.4373	7.5466
	1179.3	1212.6	2.3665	3.8895	11.4658
	1206.0	1221.2	10.3668	7.1210	1.7952
	1233.9	1228.0	0.2352	2.5069	14.4334
	1235.7				
	1269.7				
	1272.0				
^{6}F	8012.4				
	8143.4				
	8148.2				
	8341.1				
	8364.1				
	8367.0				
	8394.2				
^{6}P	34077.3				
	35520.2				
	35527.9				

Table S17: CASSCF-SO computed electronic states along with the corresponding g-tensor values for complexes $\mathbf{4_{Cl}}$ and $\mathbf{5_{Cl}}$. All the energies are reported in cm^{-1}.

	4_{Cl}					5_{Cl}				
	Spin-free states	**SOC states ($^6H_{15/2}$)**	**g-values** $g_{xx}; g_{yy}; g_{zz}$			**Spin-free states**	**SOC states ($^6H_{15/2}$)**	**g-values** $g_{xx}; g_{yy}; g_{zz}$		
^{6}H	0.0	0.0	0.0005	0.0006	19.9065	0.0	0.0	0.0003	0.0004	19.9094
	1.2	366.4	0.0166	0.0195	17.0398	0.0	389.3	0.0172	0.0190	17.0362
	583.6	662.2	0.2000	0.2357	14.1929	628.9	711.5	0.0710	0.0784	14.2275
	604.5	860.0	1.9287	2.4332	10.7432	642.5	934.3	1.7951	2.1743	11.0573
	910.3	942.9	3.4067	4.0970	13.9480	996.1	1043.0	9.2195	5.9871	1.7879
	943.0	997.7	0.5206	0.7962	12.9197	1049.1	1072.4	0.8218	3.6987	10.9060
	963.8	1143.1	0.0339	0.0416	16.7190	1066.0	1191.6	0.0700	0.2596	16.6122
	1112.4	1233.6	0.0517	0.1207	19.3538	1164.5	1265.2	0.0802	0.2380	19.2359
	1138.2					1201.3				
	1259.9					1290.3				
	1268.9					1301.7				
^{6}F	7936.1					7973.0				
	8025.0					8087.0				
	8065.4					8112.1				
	8213.8					8267.9				
	8236.9					8302.7				
	8275.2					8331.1				
	8300.8					8351.7				
^{6}P	34088.1					34081.1				
	35218.2					35329.3				
	35527.4					35552.0				

SUPPORTING INFORMATION

Table S18: CASSCF-SO computed electronic states along with the corresponding g-tensor values for complexes $\mathbf{2_{OSiPh3}}$ and $\mathbf{2_{OtBu}}$. All the energies are reported in cm^{-1}.

	2_{OSiPh3}					2_{OtBu}				
	Spin-free states	**SOC states ($^6H_{15/2}$)**	**g-values** g_{xx};	g_{yy};	g_{zz}	**Spin-free states**	**SOC states ($^6H_{15/2}$)**	**g-values** g_{xx};	g_{yy};	g_{zz}
^{6}H	0.0	0.0	0.0001	0.0001	19.9049	0.0	0	0.0000	0.0000	19.9130
	2.4	660.1	0.0115	0.0122	16.8464	0.3	833.99	0.0052	0.0053	16.7242
	1156.7	1241.6	0.0423	0.0459	13.9487	1578	1559.27	0.0033	0.0053	13.8046
	1179.2	1675.2	0.7237	0.8097	11.0998	1582.1	2101.02	0.1056	0.1117	11.1394
	1872.5	1903.4	5.3751	6.5948	8.7957	2377.4	2397.26	5.9227	6.0617	7.3204
	1900.8	1964.4	0.1571	0.6900	18.0540	2395.9	2509.84	1.1373	6.1760	14.4334
	1958.9	2008.2	1.6377	3.4017	14.9172	2495.8	2527.39	0.6156	3.1382	9.8689
	2008.6	2049.0	0.5205	2.2836	15.6530	2508.6	2534.07	10.9462	6.1256	0.6744
	2057.2					2525.8				
	2153.7					2658.9				
	2160.0					2662.2				
^{6}F	8570.6					9084.5				
	8759.9					9228.4				
	8797.3					9234.9				
	9036.8					9553.6				
	9114.7					9619.5				
	9147.2					9666.6				
	9153.9					9667.6				
^{6}P	33992.4					34023.4				
	36411.4					37153.7				
	36477.0					37170.8				

Table S19: SINGLE_ANISO computed crystal field parameters for $\mathbf{1_X}$-$\mathbf{5_X}$.

k	q	B_k^q			
		$\mathbf{1_F}$	$\mathbf{1_{Cl}}$	$\mathbf{1_{Br}}$	$\mathbf{1_I}$
2	-2	-7.01E-01	2.62E-03	1.38E-01	-3.97E-01
2	-1	4.01E-02	-7.13E-02	-6.90E-01	-1.54E+00
2	0	**-2.66E+01**	**-1.50E+01**	**-1.24E+01**	**-9.52E+00**
2	1	1.24E+00	-1.35E-02	1.62E+00	-2.88E-01
2	2	-2.37E+00	4.14E-02	-2.02E-01	-1.15E-01
4	-4	1.96E-04	9.26E-05	-2.68E-03	-5.95E-03
4	-3	2.89E-04	-1.12E-03	-3.00E-03	6.88E-03
4	-2	-2.05E-02	4.45E-05	5.53E-04	2.89E-03
4	-1	-2.85E-04	1.15E-03	1.13E-02	2.57E-02
4	0	**-1.29E-01**	**-6.15E-02**	**-5.37E-02**	**-4.34E-02**
4	1	-2.36E-02	2.11E-04	-2.71E-02	3.69E-03
4	2	-7.70E-02	-1.71E-04	-5.11E-03	3.00E-03
4	3	1.91E-02	-3.63E-04	9.42E-03	-2.00E-03
4	4	-3.11E-03	1.28E-03	2.32E-03	3.21E-03
6	-6	-1.79E-03	-4.80E-03	**8.66E-03**	**-2.22E-03**
6	-5	6.06E-04	-1.52E-04	-4.56E-03	3.96E-03
6	-4	8.46E-05	1.28E-06	3.58E-05	-9.49E-05
6	-3	1.53E-05	-9.83E-06	-2.30E-05	3.59E-05
6	-2	8.56E-04	3.29E-06	-2.42E-04	3.65E-04
6	-1	-2.17E-05	1.24E-05	1.38E-04	3.71E-04
6	0	1.24E-03	5.41E-04	3.00E-04	1.71E-04
6	1	-1.73E-05	2.77E-06	-3.17E-04	1.14E-04
6	2	3.13E-03	-7.16E-06	3.55E-04	2.87E-05
6	3	2.87E-04	-3.49E-06	9.43E-05	-4.36E-05
6	4	7.79E-06	2.21E-05	4.25E-05	1.62E-04
6	5	3.41E-03	-6.45E-05	-8.89E-04	-1.61E-03
6	6	**-9.97E-03**	**7.40E-03**	5.74E-03	-1.03E-02
8	-8	-2.91E-06	3.06E-08	3.79E-07	-9.15E-07

8	-7	1.08E-06	6.71E-08	-1.28E-06	-1.89E-06
8	-6	-9.51E-06	-1.35E-05	2.09E-05	-4.20E-06
8	-5	9.19E-06	-1.17E-06	**-3.03E-05**	**2.04E-05**
8	-4	6.04E-07	9.72E-09	2.41E-07	-4.03E-07
8	-3	-4.87E-07	-1.33E-07	-1.67E-07	5.07E-07
8	-2	5.47E-06	2.68E-08	-1.06E-06	1.44E-06
8	-1	-5.14E-08	4.46E-08	3.56E-07	6.35E-07
8	0	4.96E-07	1.06E-07	-6.62E-08	-8.90E-08
8	1	-1.15E-06	8.78E-09	-8.21E-07	1.26E-07
8	2	1.94E-05	-7.21E-08	1.05E-06	3.75E-07
8	3	**5.36E-06**	-4.56E-08	9.34E-07	-3.77E-07
8	4	-2.07E-06	1.56E-07	2.76E-07	6.65E-07
8	5	5.16E-05	-4.96E-07	-5.89E-06	-8.18E-06
8	6	-5.24E-05	**2.09E-05**	1.39E-05	-1.94E-05
8	7	2.86E-06	6.35E-08	-1.88E-06	-5.58E-07
8	8	-5.91E-06	-6.80E-08	6.48E-07	4.75E-09
10	-10	1.61E-08	-3.53E-09	2.31E-09	2.64E-08
10	-9	1.99E-08	-2.35E-09	-7.85E-09	3.19E-09
10	-8	2.95E-07	-9.88E-10	-4.65E-08	6.97E-08
10	-7	-6.86E-08	-1.39E-09	5.59E-08	9.65E-08
10	-6	1.00E-07	1.41E-07	**-1.62E-07**	2.84E-08
10	-5	-2.73E-08	3.33E-09	6.02E-08	-3.27E-08
10	-4	-7.41E-08	-2.10E-10	-2.88E-08	-7.38E-09
10	-3	-1.18E-08	1.22E-09	2.47E-08	-1.04E-09
10	-2	-4.49E-08	-5.46E-11	5.22E-09	-6.72E-09
10	-1	2.14E-09	4.43E-11	-1.85E-09	-5.53E-09
10	0	-2.15E-08	-5.94E-09	-2.74E-09	-1.28E-09
10	1	-8.07E-09	-2.61E-12	4.33E-09	-2.38E-09
10	2	-1.63E-07	8.19E-11	-8.60E-09	-7.40E-10
10	3	-1.81E-07	4.24E-10	-1.83E-08	-1.16E-08
10	4	1.21E-07	-3.67E-09	-8.17E-09	-1.25E-08
10	5	-1.52E-07	1.43E-09	1.21E-08	1.11E-08
10	6	5.47E-07	**-2.17E-07**	-1.07E-07	**1.34E-07**
10	7	-1.17E-07	-1.49E-09	7.30E-08	2.78E-08
10	8	**6.23E-07**	3.80E-10	-9.56E-08	-1.86E-08
10	9	2.29E-08	-2.36E-09	7.50E-09	1.89E-08
10	10	4.76E-08	6.62E-09	1.76E-08	-1.79E-08

The CF parameters were computed using the following equation, $\hat{H}_{CF} = \Sigma \sum_{k=-q}^{q} B_k^q O_k^q$ and here B_k^q and O_k^q are the crystal field parameters and Steven's operator, respectively.

k	q	B_k^q			
		2_F	**2_{Cl}**	**2_{Br}**	**2_I**
2	-2	1.21E+00	-1.10E-02	-1.33E-02	1.27E-01
2	-1	1.37E+00	-4.60E-01	-3.79E-02	1.60E-01
2	0	**-2.81E+01**	**-1.69E+01**	**-1.40E+01**	**-1.10E+01**
2	1	-1.43E-01	-5.48E-01	-1.66E-01	3.79E-02
2	2	2.11E+00	-2.41E-02	2.45E-02	-2.93E-02
4	-4	-1.17E-03	-2.58E-04	2.07E-04	1.24E-03
4	-3	2.21E-03	1.60E-04	-1.30E-04	-1.30E-04
4	-2	3.98E-02	-1.31E-03	2.01E-04	-5.32E-04
4	-1	-2.47E-02	6.03E-03	4.96E-04	-1.96E-03
4	0	**-1.27E-01**	**-6.25E-02**	**-4.93E-02**	**-3.72E-02**
4	1	3.31E-03	7.44E-03	1.94E-03	-4.83E-04
4	2	6.98E-02	-8.56E-04	-2.13E-04	5.23E-05
4	3	-1.20E-03	-4.83E-05	-1.17E-05	-3.90E-05
4	4	-3.51E-03	7.09E-04	6.43E-04	6.46E-05

6	-6	4.68E-03	-4.21E-03	4.92E-03	-3.66E-03
6	-5	1.77E-03	9.79E-05	2.69E-04	-2.43E-04
6	-4	9.80E-05	-1.09E-07	4.97E-06	2.88E-05
6	-3	-8.89E-05	-1.36E-06	-3.95E-06	-2.05E-06
6	-2	-1.54E-03	3.51E-05	-3.66E-06	-1.45E-05
6	-1	-8.23E-05	1.59E-04	1.33E-05	-6.96E-05
6	0	1.23E-03	4.64E-04	2.58E-04	8.51E-05
6	1	-1.81E-05	1.75E-04	7.45E-05	-1.48E-05
6	2	-2.67E-03	3.23E-05	7.61E-07	5.24E-06
6	3	6.35E-05	-1.37E-07	-5.78E-07	-7.86E-07
6	4	-6.31E-05	1.03E-05	1.36E-05	3.68E-07
6	5	-1.33E-03	-1.20E-03	-1.85E-04	2.17E-04
6	6	**5.06E-03**	**-5.68E-03**	**-5.20E-03**	**-6.31E-03**
8	-8	-4.13E-06	-7.58E-08	-3.32E-08	1.52E-07
8	-7	-1.03E-06	-6.90E-07	1.02E-07	1.65E-07
8	-6	2.51E-05	-1.30E-05	1.23E-05	-7.10E-06
8	-5	2.75E-05	8.07E-07	1.83E-06	-1.27E-06
8	-4	7.25E-08	-6.55E-09	3.12E-08	1.43E-07
8	-3	2.92E-07	1.92E-08	-3.67E-08	-1.72E-08
8	-2	-1.05E-05	8.98E-08	-4.76E-09	-9.68E-08
8	-1	-1.41E-06	3.88E-07	2.46E-08	-8.50E-08
8	0	6.62E-07	6.93E-08	-3.92E-08	-8.99E-08
8	1	7.32E-08	4.47E-07	1.23E-07	-1.90E-08
8	2	-1.80E-05	1.18E-07	-1.28E-08	2.64E-08
8	3	-4.80E-07	-4.46E-09	-4.86E-09	-9.17E-09
8	4	-2.24E-06	7.66E-08	8.75E-08	2.45E-09
8	5	-2.03E-05	-1.02E-05	-1.25E-06	1.14E-06
8	6	**2.74E-05**	**-1.75E-05**	**-1.31E-05**	**-1.22E-05**
8	7	1.56E-06	-1.54E-07	-1.66E-07	-6.11E-08
8	8	-1.31E-06	-1.67E-08	1.31E-08	-1.44E-07
10	-10	-2.88E-08	-8.90E-10	1.24E-09	-4.01E-09
10	-9	3.82E-09	-5.96E-10	-4.22E-10	2.24E-10
10	-8	**4.06E-07**	8.84E-09	-1.14E-09	-6.12E-10
10	-7	4.24E-08	4.78E-08	-9.39E-09	-1.50E-08
10	-6	-2.38E-07	9.97E-08	-7.24E-08	2.55E-08
10	-5	-7.74E-08	-1.24E-09	-1.72E-09	1.45E-10
10	-4	-5.98E-08	1.83E-10	-4.60E-10	-1.69E-09
10	-3	8.75E-08	2.33E-10	3.59E-10	1.23E-10
10	-2	7.74E-08	-8.83E-10	7.75E-11	2.05E-10
10	-1	-5.60E-09	-2.37E-09	-2.28E-10	1.20E-09
10	0	-1.96E-08	-4.54E-09	-1.87E-09	-1.42E-10
10	1	9.08E-10	-2.45E-09	-1.31E-09	2.55E-10
10	2	1.31E-07	-9.04E-10	-1.30E-11	-7.06E-11
10	3	-4.51E-08	2.51E-10	3.33E-11	-1.82E-11
10	4	1.02E-07	-4.41E-10	-1.51E-09	-8.30E-11
10	5	5.84E-08	1.75E-08	1.07E-09	-1.20E-10
10	6	-2.64E-07	**1.35E-07**	**7.66E-08**	**4.40E-08**
10	7	-8.50E-08	9.39E-09	1.39E-08	5.04E-09
10	8	1.28E-07	5.18E-10	-2.46E-10	1.18E-09
10	9	-4.98E-08	-1.88E-10	-1.12E-09	4.77E-10
10	10	-6.18E-09	-2.88E-09	-2.52E-09	1.70E-09

The CF parameters were computed using the following equation, $\hat{H}_{CF} = \Sigma \sum_{k=-q}^{q} B_k^q O_k^q$ and here B_k^q and O_k^q are the crystal field parameters and Steven's operator, respectively.

k	q	B_k^q		
		3_{Cl}	**4_{Cl}**	**5_{Cl}**

2	-2	-7.88E-02	-3.05E-01	7.11E-01
2	-1	6.64E-02	3.04E+00	-8.74E-02
2	0	**-1.69E+01**	**-1.52E+01**	**-1.61E+01**
2	1	-1.05E+00	-6.62E-02	-2.86E+00
2	2	-1.34E-01	-6.05E+00	4.39E+00
4	-4	-6.18E-04	-2.04E-03	-1.40E-03
4	-3	6.29E-04	-1.40E-02	-6.26E-04
4	-2	-4.86E-04	3.64E-04	-4.83E-03
4	-1	-8.09E-04	**-5.79E-02**	1.73E-03
4	0	**-5.90E-02**	-4.93E-02	**-5.56E-02**
4	1	1.65E-02	1.49E-03	5.60E-02
4	2	-4.44E-03	4.42E-02	-3.06E-02
4	3	5.65E-04	-3.89E-04	-1.57E-02
4	4	-8.58E-04	-2.71E-02	-1.24E-02
6	-6	4.33E-03	8.29E-04	-2.75E-03
6	-5	1.18E-03	**9.31E-03**	-3.20E-03
6	-4	-6.46E-07	-8.61E-05	-1.21E-04
6	-3	-1.34E-06	-5.17E-04	-8.42E-05
6	-2	4.05E-05	1.25E-05	1.13E-04
6	-1	-2.53E-05	8.90E-05	-1.22E-05
6	0	4.76E-04	3.44E-04	4.45E-04
6	1	1.68E-04	-2.18E-05	-2.17E-04
6	2	1.46E-04	-4.16E-04	5.08E-04
6	3	-4.88E-06	4.50E-05	-3.71E-04
6	4	-3.47E-05	-8.62E-04	-3.79E-04
6	5	-1.07E-03	-9.42E-04	**-7.99E-03**
6	6	**-3.46E-03**	7.23E-03	-6.33E-03
8	-8	1.29E-07	1.37E-06	3.07E-06
8	-7	5.46E-07	1.10E-05	3.65E-06
8	-6	1.31E-05	2.10E-06	-7.85E-06
8	-5	1.00E-05	6.83E-05	-2.56E-05
8	-4	1.23E-08	-5.79E-07	-9.53E-07
8	-3	5.25E-08	-4.81E-06	-7.02E-07
8	-2	2.33E-07	1.55E-07	6.78E-08
8	-1	-5.81E-08	-8.79E-07	7.86E-09
8	0	1.30E-07	7.08E-08	1.26E-07
8	1	6.57E-07	4.01E-09	8.61E-07
8	2	4.72E-07	2.71E-06	-9.51E-07
8	3	7.55E-08	4.06E-07	-3.84E-06
8	4	-2.71E-07	-6.34E-06	-3.15E-06
8	5	-9.07E-06	-6.85E-06	-6.36E-05
8	6	-1.05E-05	1.86E-05	-1.81E-05
8	7	-3.97E-07	-1.75E-06	5.65E-06
8	8	-2.37E-07	7.94E-06	4.73E-06
10	-10	-9.22E-10	-2.10E-08	3.61E-08
10	-9	6.37E-10	**-2.30E-07**	1.78E-08
10	-8	-1.27E-08	2.10E-08	7.84E-08
10	-7	-1.85E-08	8.86E-08	1.46E-08
10	-6	**-1.03E-07**	-1.48E-08	6.13E-08
10	-5	-2.14E-08	-1.40E-07	6.20E-08
10	-4	-4.12E-09	1.32E-08	2.22E-08
10	-3	-2.63E-10	1.29E-07	2.54E-08
10	-2	-9.97E-10	-1.96E-10	-3.76E-09
10	-1	3.28E-10	-7.41E-09	7.97E-11
10	0	-4.43E-09	-2.63E-09	-3.87E-09
10	1	-1.41E-11	8.01E-10	1.23E-08
10	2	-3.95E-09	1.48E-08	-1.91E-08
10	3	2.77E-09	-1.06E-08	1.13E-07
10	4	6.99E-09	1.22E-07	7.62E-08
10	5	1.88E-08	1.33E-08	**1.55E-07**

10	6	8.23E-08	-1.33E-07	1.41E-07
10	7	1.09E-08	-1.07E-09	3.24E-09
10	8	1.62E-08	1.74E-07	1.18E-07
10	9	-2.64E-09	3.29E-08	7.11E-08
10	10	2.94E-09	-1.20E-07	6.05E-08

Table S20: Selected structural parameters of reported Dy(III) based SMMs

Complex	Dy-O(18C6)	[Ref]
$[Dy(H_2O)_3(18C6)]^{3+}$	2.510	*Inorg. Chem*. 2018, **57**, 13225−13234
$[Dy(18C6)(Cl)(O^tBu)]^+$	2.550	*Inorg. Chem*. 2022, **61**, 1, 227–235
$[Dy(18\text{-}C\text{-}6)I_2]^+$	2.452	*Adv. Sci*. 2024, 2308548
$[Dy(18\text{-}C\text{-}6)(O^tBu)_2]^+$	2.613	*Adv. Sci*. 2024, 2308548
$[Dy(18\text{-}C\text{-}6)(AdO)_2]^+$	2.636	*Adv. Sci*. 2024, 2308548
	Dy-X	
$[Dy(18\text{-}C\text{-}6)I_2]^+$	3.013 (X = I)	*Adv. Sci*. 2024, 2308548
$[Dy(OtBu)Cl(18\text{-}C\text{-}6)]^+$	2.608 (X = Cl)	*Inorg. Chem*. 2022, **61**, 1, 227–235
$[DyLF]^+$	2.12 (X = F)	*Inorg. Chem.* 2022, **61**, 9906−9917
	Dy-S	
$[Dy_4\{N(SiMe_3)_2\}_4(\mu\text{-}SEt)_8(\mu_4\text{-}SEt)]$	2.9406/2.8226	*Organometallics* 2013, 32, **5**, 1224–1229
$[Dy((-)pbipy)(pdtc)_3]$	2.775(2)–2.876(2)	*Inorganica Chim. Acta*, 2018, **473**, 145–151.
$[(diethyl\text{-}dtc)_3Dy(phen)]$	2.9027/2.8066/2.8740	*Dalton Trans*., 2016,**45**, 8149-8153
$[Dy^{III}L^{ON3}(C_5H_{10}NS_2)_2]$	2.8133(5)–2.9647(6)	*Chem. Commun*., 2020,**56**, 1533-1536
$[Dy(tba)_3phen]$	2.80–2.84	*J. Mater. Chem. C*, 2022,**10**, 13946-13953
$[(dtc)_3Dy(dmbipy)]$	2.833	*Inorg. Chem. Commun*., 2018, **95**, 82–85
dtc: dithiacarbamate; tba: thiobenzoate; ptdc: pyrrolidine-dithiocarbamate		

DFT Optimised Coordinates

1_F			
Dy	0.000000000000	0.000000000000	0.000000000000
F	0.026960000000	0.442548000000	1.978647000000
F	-0.623207000000	0.410134000000	-1.888786000000
O	-2.320288000000	-1.273184000000	0.304311000000
O	-2.311032000000	1.406187000000	0.396237000000
O	0.000000000000	2.725596000000	0.000000000000
O	2.238550000000	1.331750000000	-0.476454000000
C	-3.526717000000	-0.589213000000	0.236795000000
C	-3.514948000000	0.753885000000	0.276803000000
C	-2.309282000000	2.784343000000	0.429913000000
C	-1.155272000000	3.444252000000	0.232597000000
C	1.088028000000	3.384946000000	-0.520339000000
C	2.215027000000	2.693285000000	-0.757425000000
H	-4.442289000000	-1.183133000000	0.130604000000
H	-4.428620000000	1.357663000000	0.202925000000
H	-3.258305000000	3.293156000000	0.642666000000

H	-1.078019000000	4.538393000000	0.270394000000
H	0.991851000000	4.456018000000	-0.740210000000
H	3.121123000000	3.138453000000	-1.184917000000
O	-0.022303000000	-2.621664000000	0.221959000000
O	2.275259000000	-1.313738000000	-0.185205000000
C	-2.362507000000	-2.647637000000	0.415895000000
C	-1.208717000000	-3.331905000000	0.378342000000
C	1.152861000000	-3.351517000000	0.125182000000
C	2.305462000000	-2.696179000000	-0.078367000000
C	3.473665000000	-0.658447000000	-0.442850000000
C	3.448858000000	0.674543000000	-0.593829000000
H	-3.341334000000	-3.126753000000	0.541844000000
H	-1.141876000000	-4.422516000000	0.465280000000
H	1.087318000000	-4.441854000000	0.221655000000
H	3.277939000000	-3.195333000000	-0.164894000000
H	4.384585000000	-1.264729000000	-0.508672000000
H	4.344346000000	1.275270000000	-0.794492000000

1_{Cl}

Dy	0.000000000000	0.000000000000	0.000000000000
Cl	0.000000000000	0.000000000000	2.503916000000
Cl	0.573355000000	0.462443000000	-2.400143000000
O	-1.316182000000	2.303277000000	-0.126009000000
O	1.284720000000	2.307754000000	0.424273000000
O	2.641387000000	0.021623000000	0.355488000000
O	1.376773000000	-2.231329000000	-0.252034000000
C	-0.625643000000	3.500674000000	-0.205022000000
C	0.687568000000	3.501052000000	0.076111000000
C	2.620583000000	2.324717000000	0.775394000000
C	3.306668000000	1.171275000000	0.739940000000
C	3.392155000000	-1.047227000000	-0.088173000000
C	2.755029000000	-2.187903000000	-0.397245000000
H	-1.182446000000	4.394436000000	-0.510601000000
H	1.316059000000	4.398294000000	0.019241000000
H	3.053186000000	3.279481000000	1.099694000000
H	4.360152000000	1.079247000000	1.032227000000
H	4.475420000000	-0.912026000000	-0.195626000000
H	3.257606000000	-3.084120000000	-0.779588000000
O	-2.605801000000	-0.000067000000	-0.051670000000
O	-1.253671000000	-2.287896000000	-0.072129000000
C	-2.680744000000	2.322198000000	-0.330499000000
C	-3.341598000000	1.155492000000	-0.284328000000
C	-3.307626000000	-1.181820000000	0.132387000000
C	-2.625761000000	-2.336429000000	0.121824000000
C	-0.593853000000	-3.480918000000	-0.334245000000
C	0.743415000000	-3.446631000000	-0.433838000000
H	-3.162920000000	3.288030000000	-0.524271000000
H	-4.421452000000	1.052030000000	-0.441266000000
H	-4.388045000000	-1.112691000000	0.306346000000
H	-3.085304000000	-3.318555000000	0.285124000000
H	-1.199320000000	-4.385368000000	-0.464547000000
H	1.362975000000	-4.325254000000	-0.649634000000

1_{Br}

Dy	0.000000000000	0.000000000000	0.000000000000
Br	0.000000000000	0.000000000000	2.667086000000
Br	-0.392585000000	0.654086000000	-2.562578000000

O	-2.463456000000	-0.978651000000	-0.125492000000
O	-2.105139000000	1.598279000000	0.413796000000
O	0.347711000000	2.619695000000	0.343676000000
O	2.400407000000	1.048716000000	-0.252532000000
C	-3.553250000000	-0.128344000000	-0.209344000000
C	-3.370296000000	1.172802000000	0.066005000000
C	-1.936047000000	2.926385000000	0.755172000000
C	-0.698112000000	3.443307000000	0.719183000000
C	1.512506000000	3.211166000000	-0.100317000000
C	2.552557000000	2.418874000000	-0.403505000000
H	-4.515396000000	-0.556722000000	-0.513996000000
H	-4.170372000000	1.920653000000	0.005215000000
H	-2.821403000000	3.490328000000	1.074334000000
H	-0.459403000000	4.475076000000	1.005649000000
H	1.530824000000	4.302132000000	-0.212468000000
H	3.511577000000	2.787983000000	-0.785412000000
O	-0.365299000000	-2.577639000000	-0.038083000000
O	2.086925000000	-1.561042000000	-0.058517000000
C	-2.673952000000	-2.328111000000	-0.323050000000
C	-1.612024000000	-3.145821000000	-0.270102000000
C	0.704617000000	-3.437560000000	0.158833000000
C	1.943203000000	-2.924634000000	0.148302000000
C	3.361669000000	-1.077340000000	-0.320426000000
C	3.515576000000	0.250588000000	-0.427360000000
H	-3.697709000000	-2.670461000000	-0.516618000000
H	-1.660698000000	-4.230475000000	-0.420040000000
H	0.483032000000	-4.495594000000	0.342502000000
H	2.850987000000	-3.514833000000	0.321242000000
H	4.172315000000	-1.804756000000	-0.443800000000
H	4.472702000000	0.739992000000	-0.643424000000

1_I

Dy	0.000000000000	0.000000000000	0.000000000000
I	0.478903000000	-0.409770000000	-2.824012000000
I	0.000000000000	0.000000000000	2.898363000000
O	-1.625616000000	-2.067731000000	0.187932000000
O	0.994550000000	-2.442462000000	0.245067000000
O	2.632983000000	-0.362877000000	0.163691000000
O	1.601436000000	2.084548000000	0.229819000000
C	-1.148454000000	-3.292356000000	0.629510000000
C	0.179500000000	-3.479526000000	0.658688000000
C	2.354860000000	-2.684573000000	0.152843000000
C	3.183607000000	-1.631376000000	0.109854000000
C	3.471746000000	0.693686000000	0.462759000000
C	2.952490000000	1.929454000000	0.500712000000
H	-1.880609000000	-4.038881000000	0.959062000000
H	0.656467000000	-4.398125000000	1.021106000000
H	2.685391000000	-3.727834000000	0.080252000000
H	4.271864000000	-1.713288000000	0.000085000000
H	4.525869000000	0.473114000000	0.669375000000
H	3.532599000000	2.829212000000	0.736260000000
O	-2.526738000000	0.286437000000	-0.569991000000
O	-0.931772000000	2.381843000000	-0.402544000000
C	-2.983234000000	-1.942946000000	-0.040271000000
C	-3.444286000000	-0.747398000000	-0.434731000000
C	-2.982744000000	1.491400000000	-1.082657000000

C	-2.174065000000	2.556930000000	-0.996157000000
C	-0.213726000000	3.520553000000	-0.057351000000
C	1.075488000000	3.362338000000	0.274494000000
H	-3.616187000000	-2.825744000000	0.108916000000
H	-4.498128000000	-0.527751000000	-0.640619000000
H	-3.968806000000	1.503723000000	-1.561953000000
H	-2.414756000000	3.548628000000	-1.397064000000
H	-0.747114000000	4.478054000000	-0.040887000000
H	1.731611000000	4.180484000000	0.594641000000

2_F

Dy	0.000000000000	0.000000000000	0.000000000000
F	0.445891000000	-0.149893000000	1.971435000000
F	0.555416000000	-0.098908000000	-1.955186000000
S	-3.108205000000	-0.478713000000	0.212800000000
S	-1.917573000000	2.473774000000	0.284043000000
S	1.220230000000	2.915830000000	0.236915000000
S	3.224904000000	0.444519000000	0.169835000000
C	-3.830233000000	0.824277000000	-0.721473000000
C	-3.324972000000	2.076154000000	-0.690891000000
C	-1.195727000000	3.783116000000	-0.642420000000
C	0.142387000000	3.965148000000	-0.664623000000
C	2.658254000000	2.926169000000	-0.774553000000
C	3.504108000000	1.873269000000	-0.805550000000
H	-4.755413000000	0.589985000000	-1.270851000000
H	-3.820078000000	2.908496000000	-1.215146000000
H	-1.887261000000	4.487171000000	-1.130716000000
H	0.593364000000	4.824219000000	-1.186000000000
H	2.869674000000	3.854562000000	-1.327012000000
H	4.429395000000	1.907660000000	-1.401806000000
S	-1.109986000000	-2.942577000000	0.070006000000
S	2.044103000000	-2.513002000000	0.079753000000
C	-3.454302000000	-1.878174000000	-0.794699000000
C	-2.600362000000	-2.922457000000	-0.856372000000
C	-0.051437000000	-3.879474000000	-0.976857000000
C	1.286119000000	-3.690980000000	-0.973213000000
C	3.449668000000	-2.056080000000	-0.866875000000
C	3.949922000000	-0.802342000000	-0.828520000000
H	-4.430672000000	-1.896269000000	-1.303618000000
H	-2.847654000000	-3.830894000000	-1.428045000000
H	-0.525455000000	-4.667967000000	-1.581274000000
H	1.947790000000	-4.317233000000	-1.592095000000
H	3.947359000000	-2.854585000000	-1.439365000000
H	4.871101000000	-0.539041000000	-1.371910000000

2_{Cl}

Dy	0.000000000000	0.000000000000	0.000000000000
Cl	0.000000000000	0.000000000000	2.536021000000
Cl	0.255748000000	-0.054183000000	-2.532456000000
S	-3.167246000000	0.144052000000	0.074935000000
S	-1.467256000000	2.807279000000	0.089653000000
S	1.692814000000	2.670466000000	0.152148000000
S	3.153421000000	-0.140801000000	0.201528000000
C	-3.631760000000	1.516964000000	-0.908199000000
C	-2.903853000000	2.657383000000	-0.901363000000
C	-0.493558000000	3.920174000000	-0.848719000000
C	0.857688000000	3.861062000000	-0.822806000000

C	3.137277000000	2.380912000000	-0.793361000000
C	3.760260000000	1.180034000000	-0.773054000000
H	-4.564244000000	1.433921000000	-1.487746000000
H	-3.218984000000	3.542507000000	-1.475500000000
H	-1.024314000000	4.699615000000	-1.417201000000
H	1.473849000000	4.590374000000	-1.371431000000
H	3.542770000000	3.226973000000	-1.369612000000
H	4.692189000000	1.009581000000	-1.334128000000
S	-1.715280000000	-2.659326000000	0.150181000000
S	1.442128000000	-2.808755000000	0.212797000000
C	-3.759994000000	-1.205080000000	-0.871654000000
C	-3.138133000000	-2.406309000000	-0.839049000000
C	-0.849342000000	-3.878460000000	-0.760786000000
C	0.501902000000	-3.941466000000	-0.734781000000
C	2.904827000000	-2.671721000000	-0.738689000000
C	3.634716000000	-1.532427000000	-0.744234000000
H	-4.686040000000	-1.051565000000	-1.447138000000
H	-3.535792000000	-3.274302000000	-1.387534000000
H	-1.448789000000	-4.619962000000	-1.311441000000
H	1.048827000000	-4.736257000000	-1.265561000000
H	3.229953000000	-3.562585000000	-1.298112000000
H	4.576512000000	-1.459502000000	-1.309923000000

2_{Br}

Dy	0.000000000000	0.000000000000	0.000000000000
Br	0.000000000000	0.000000000000	2.691825000000
Br	0.007277000000	-0.001008000000	-2.699068000000
S	-3.162896000000	0.078496000000	0.114130000000
S	-1.514617000000	2.773313000000	0.120713000000
S	1.648426000000	2.697386000000	0.088545000000
S	3.156164000000	-0.081712000000	0.084082000000
C	-3.677141000000	1.452726000000	-0.839949000000
C	-2.972454000000	2.607055000000	-0.835232000000
C	-0.590557000000	3.911840000000	-0.836260000000
C	0.761028000000	3.878163000000	-0.852068000000
C	3.063972000000	2.437451000000	-0.908908000000
C	3.708682000000	1.248764000000	-0.910963000000
H	-4.621003000000	1.357139000000	-1.398635000000
H	-3.318020000000	3.493464000000	-1.389391000000
H	-1.152475000000	4.686364000000	-1.380939000000
H	1.347787000000	4.623930000000	-1.410581000000
H	3.433820000000	3.293116000000	-1.494661000000
H	4.626510000000	1.094120000000	-1.498956000000
S	-1.656590000000	-2.691451000000	0.139990000000
S	1.503007000000	-2.778611000000	0.138516000000
C	-3.738862000000	-1.267741000000	-0.844726000000
C	-3.093266000000	-2.456336000000	-0.832678000000
C	-0.785765000000	-3.892824000000	-0.789387000000
C	0.565942000000	-3.930170000000	-0.790222000000
C	2.945323000000	-2.619922000000	-0.841582000000
C	3.651052000000	-1.466653000000	-0.865908000000
H	-4.671337000000	-1.125359000000	-1.412425000000
H	-3.477402000000	-3.324887000000	-1.389600000000
H	-1.382240000000	-4.646701000000	-1.326198000000
H	1.118793000000	-4.715919000000	-1.328137000000
H	3.281054000000	-3.510388000000	-1.395319000000

H	4.585883000000	-1.377844000000	-1.440775000000

2_I

Dy	0.000000000000	0.000000000000	0.000000000000
I	0.000000000000	0.000000000000	2.913244000000
I	0.000101000000	-0.001214000000	-2.911116000000
S	-3.160825000000	-0.055603000000	0.084572000000
S	-1.619247000000	2.694792000000	0.122797000000
S	1.539216000000	2.746770000000	0.127845000000
S	3.154182000000	0.043962000000	0.112474000000
C	-3.720777000000	1.304285000000	-0.866889000000
C	-3.061441000000	2.483512000000	-0.849337000000
C	-0.733284000000	3.881905000000	-0.812471000000
C	0.617616000000	3.903430000000	-0.811530000000
C	2.984374000000	2.568819000000	-0.846915000000
C	3.676855000000	1.408637000000	-0.854253000000
H	-4.658617000000	1.174557000000	-1.428684000000
H	-3.435820000000	3.362849000000	-1.395848000000
H	-1.322307000000	4.640336000000	-1.350941000000
H	1.182623000000	4.680641000000	-1.349035000000
H	3.331008000000	3.452690000000	-1.404231000000
H	4.616040000000	1.299188000000	-1.418113000000
S	-1.546639000000	-2.754422000000	0.092191000000
S	1.608587000000	-2.708537000000	0.115881000000
C	-3.680204000000	-1.413611000000	-0.892409000000
C	-2.986999000000	-2.573370000000	-0.888272000000
C	-0.620466000000	-3.908162000000	-0.845522000000
C	0.730452000000	-3.889063000000	-0.834979000000
C	3.057275000000	-2.487753000000	-0.843909000000
C	3.717850000000	-1.309086000000	-0.847201000000
H	-4.617388000000	-1.300564000000	-1.458784000000
H	-3.330080000000	-3.455163000000	-1.451016000000
H	-1.183168000000	-4.681119000000	-1.391403000000
H	1.322595000000	-4.646319000000	-1.371742000000
H	3.434253000000	-3.361931000000	-1.396883000000
H	4.659254000000	-1.176484000000	-1.402392000000

3_{Cl}

Dy	0.000000000000	0.000000000000	0.000000000000
Cl	0.000000000000	0.000000000000	2.544938000000
Cl	-0.456727000000	0.128008000000	-2.495154000000
Se	-3.326147000000	-0.105112000000	0.433413000000
Se	-1.750915000000	2.825753000000	0.385092000000
Se	1.567185000000	2.932135000000	0.192987000000
Se	3.313157000000	0.102861000000	0.071358000000
C	-3.935339000000	1.326733000000	-0.656815000000
C	-3.297071000000	2.513961000000	-0.675809000000
C	-0.867951000000	4.031686000000	-0.789529000000
C	0.476742000000	4.074136000000	-0.869073000000
C	2.995370000000	2.703486000000	-1.044171000000
C	3.702658000000	1.557514000000	-1.094199000000
H	-4.848661000000	1.145611000000	-1.244907000000
H	-3.659308000000	3.361084000000	-1.279292000000
H	-1.508886000000	4.712617000000	-1.371362000000
H	1.002780000000	4.793832000000	-1.515894000000
H	3.238444000000	3.568345000000	-1.681409000000
H	4.559909000000	1.427178000000	-1.773303000000

Se	-1.569922000000	-2.922757000000	0.317363000000
Se	1.746770000000	-2.832496000000	0.159832000000
C	-3.834321000000	-1.538113000000	-0.706399000000
C	-3.122134000000	-2.681823000000	-0.754071000000
C	-0.607360000000	-4.067966000000	-0.857662000000
C	0.738327000000	-4.031650000000	-0.922116000000
C	3.172361000000	-2.506817000000	-1.059651000000
C	3.805878000000	-1.318078000000	-1.096578000000
H	-4.751747000000	-1.396963000000	-1.299024000000
H	-3.423622000000	-3.532851000000	-1.384718000000
H	-1.201806000000	-4.786370000000	-1.443857000000
H	1.313318000000	-4.719190000000	-1.562299000000
H	3.479377000000	-3.352543000000	-1.695069000000
H	4.662288000000	-1.131476000000	-1.763580000000

4_{Cl}

Dy	0.000000000000	0.000000000000	0.000000000000
Cl	0.005213000000	-1.183490000000	-2.269224000000
Cl	0.000000000000	0.000000000000	2.544531000000
S	-2.910708000000	-0.117792000000	-0.579749000000
O	-1.334851000000	-2.422810000000	0.535222000000
O	1.446742000000	-2.357285000000	0.516273000000
S	2.908933000000	0.029392000000	-0.602000000000
C	-3.480535000000	-1.420583000000	0.447791000000
C	-2.673565000000	-2.432677000000	0.830735000000
C	-0.589195000000	-3.516411000000	0.903393000000
C	0.757760000000	-3.485093000000	0.893401000000
C	2.790284000000	-2.310500000000	0.786542000000
C	3.546745000000	-1.261437000000	0.400994000000
H	-4.543197000000	-1.434320000000	0.729301000000
H	-3.038190000000	-3.295726000000	1.408260000000
H	-1.132830000000	-4.424166000000	1.197090000000
H	1.347841000000	-4.366317000000	1.178015000000
H	3.202841000000	-3.163191000000	1.346995000000
H	4.613908000000	-1.234563000000	0.664203000000
O	-1.445238000000	2.386516000000	0.079579000000
O	1.322289000000	2.449577000000	0.085908000000
C	-3.553719000000	1.299471000000	0.237191000000
C	-2.785255000000	2.389113000000	0.425531000000
C	-0.760004000000	3.578030000000	0.239901000000
C	0.582619000000	3.608612000000	0.243440000000
C	2.657952000000	2.511135000000	0.443553000000
C	3.478263000000	1.462210000000	0.243334000000
H	-4.610949000000	1.312034000000	0.538284000000
H	-3.161909000000	3.321122000000	0.872145000000
H	-1.357597000000	4.493549000000	0.338224000000
H	1.137283000000	4.550399000000	0.344793000000
H	2.985536000000	3.451739000000	0.910277000000
H	4.530941000000	1.518666000000	0.555067000000

5_{Cl}

Dy	0.000000000000	0.000000000000	0.000000000000
Cl	0.000000000000	0.000000000000	2.522020000000
Cl	-0.104449000000	0.997859000000	-2.292262000000
Se	-3.012856000000	-0.505282000000	0.587314000000
O	-1.567285000000	2.219207000000	0.528015000000
O	1.170935000000	2.450445000000	0.502726000000

Se	3.042235000000	0.022910000000	0.568517000000
C	-3.643281000000	1.199902000000	0.001296000000
C	-2.877664000000	2.299218000000	0.100809000000
C	-0.958528000000	3.405811000000	0.893262000000
C	0.378968000000	3.520105000000	0.880032000000
C	2.430196000000	2.745270000000	0.020247000000
C	3.366562000000	1.787433000000	-0.085929000000
H	-4.674096000000	1.267561000000	-0.371822000000
H	-3.230774000000	3.306257000000	-0.170262000000
H	-1.610156000000	4.220773000000	1.234384000000
H	0.891228000000	4.433362000000	1.209624000000
H	2.593344000000	3.789359000000	-0.288710000000
H	4.356866000000	2.009030000000	-0.505797000000
O	-1.176225000000	-2.279218000000	-1.068625000000
O	1.553587000000	-2.076969000000	-1.057598000000
C	-3.413347000000	-1.478679000000	-1.008512000000
C	-2.472920000000	-2.249014000000	-1.574393000000
C	-0.394650000000	-3.349012000000	-1.480345000000
C	0.942545000000	-3.250833000000	-1.474064000000
C	2.842668000000	-1.863230000000	-1.529967000000
C	3.634619000000	-0.933161000000	-0.976127000000
H	-4.428608000000	-1.429449000000	-1.424658000000
H	-2.642381000000	-2.869355000000	-2.467551000000
H	-0.914948000000	-4.276280000000	-1.753129000000
H	1.595675000000	-4.092003000000	-1.740083000000
H	3.137694000000	-2.485253000000	-2.388825000000
H	4.643837000000	-0.744810000000	-1.366375000000

2_{OtBu}

Dy	0.000000000000	0.000000000000	0.000000000000
S	-2.659881000000	1.440373000000	0.367162000000
S	-0.080433000000	3.127428000000	-0.036811000000
S	2.723687000000	1.793026000000	-0.114926000000
S	2.908378000000	-1.343414000000	-0.084228000000
C	-2.670442000000	2.830312000000	-0.711534000000
C	-1.548590000000	3.555266000000	-0.892109000000
C	1.155320000000	3.737098000000	-1.125076000000
C	2.374979000000	3.161416000000	-1.154231000000
C	3.949050000000	0.959212000000	-1.051652000000
C	4.026225000000	-0.387188000000	-1.039671000000
H	-3.637219000000	3.114006000000	-1.153955000000
H	-1.536123000000	4.468521000000	-1.506371000000
H	0.916417000000	4.644654000000	-1.699842000000
H	3.195155000000	3.564546000000	-1.768015000000
H	4.690931000000	1.577668000000	-1.580733000000
H	4.834446000000	-0.928500000000	-1.555591000000
S	-2.466803000000	-1.700897000000	0.452008000000
S	0.322793000000	-3.053822000000	0.089381000000
C	-3.909235000000	0.442370000000	-0.357715000000
C	-3.827611000000	-0.902007000000	-0.321077000000
C	-2.294491000000	-3.127414000000	-0.561891000000
C	-1.088479000000	-3.706321000000	-0.722487000000
C	1.607480000000	-3.508063000000	-1.020710000000
C	2.731661000000	-2.766726000000	-1.091873000000
H	-4.793706000000	0.961124000000	-0.758989000000
H	-4.640590000000	-1.547893000000	-0.687114000000

H	-3.216035000000	-3.558363000000	-0.981619000000
H	-0.959149000000	-4.641969000000	-1.287622000000
H	1.483789000000	-4.452625000000	-1.571450000000
H	3.586273000000	-3.062463000000	-1.719341000000
C	0.856635000000	0.402515000000	3.268877000000
O	0.425221000000	0.181508000000	1.932720000000
C	0.058945000000	0.029591000000	-3.402284000000
O	0.000000000000	0.000000000000	-1.987696000000
C	0.861332000000	1.918956000000	3.526976000000
H	-0.153056000000	2.339512000000	3.371296000000
H	1.181489000000	2.158357000000	4.561082000000
H	1.557409000000	2.425448000000	2.826793000000
C	2.273722000000	-0.177124000000	3.420351000000
H	2.661881000000	-0.047263000000	4.450598000000
H	2.272560000000	-1.260027000000	3.182457000000
H	2.973330000000	0.330910000000	2.724688000000
C	-0.127642000000	-0.311158000000	4.209884000000
H	-1.151895000000	0.090038000000	4.067724000000
H	-0.146689000000	-1.397709000000	3.988062000000
H	0.152189000000	-0.178556000000	5.274433000000
C	-0.338222000000	1.440663000000	-3.868974000000
H	-0.315055000000	1.535003000000	-4.973640000000
H	-1.361913000000	1.682492000000	-3.517530000000
H	0.359492000000	2.187867000000	-3.438751000000
C	-0.926669000000	-1.024317000000	-3.936445000000
H	-0.941523000000	-1.056028000000	-5.044744000000
H	-0.644397000000	-2.029349000000	-3.561180000000
H	-1.952107000000	-0.798623000000	-3.578412000000
C	1.497924000000	-0.301216000000	-3.832839000000
H	2.201752000000	0.445760000000	-3.413511000000
H	1.786268000000	-1.299768000000	-3.445594000000
H	1.607902000000	-0.307603000000	-4.936161000000

2_{OSiPh3}

Dy	0.000000000000	0.000000000000	0.000000000000
Si	-0.650218000000	-1.030599000000	3.159793000000
Si	0.947021000000	1.333177000000	-3.229795000000
O	0.000000000000	0.000000000000	2.028960000000
O	0.618643000000	0.987199000000	-1.649379000000
S	-2.831971000000	0.661037000000	-0.569392000000
S	-0.923705000000	2.870723000000	0.825684000000
S	2.250391000000	2.525189000000	0.842844000000
S	2.920014000000	-0.381009000000	0.428253000000
C	-3.141352000000	2.382953000000	-0.703927000000
C	-2.364639000000	3.295180000000	-0.086159000000
C	0.160220000000	4.105125000000	0.182538000000
C	1.498613000000	3.940425000000	0.141181000000
C	3.455123000000	2.110929000000	-0.365007000000
C	3.782478000000	0.812988000000	-0.534601000000
H	-4.066848000000	2.665586000000	-1.228228000000
H	-2.636881000000	4.363415000000	-0.104767000000
H	-0.311858000000	5.042433000000	-0.151940000000
H	2.161056000000	4.720706000000	-0.262995000000
H	3.926041000000	2.918624000000	-0.945668000000
H	4.556047000000	0.467863000000	-1.234259000000
S	-1.752662000000	-2.032737000000	-1.096201000000

SUPPORTING INFORMATION

S	0.994627000000	-2.891168000000	0.223022000000
C	-2.819496000000	0.110755000000	-2.249797000000
C	-2.306656000000	-1.112813000000	-2.497969000000
C	-0.829596000000	-3.368146000000	-1.749732000000
C	0.309314000000	-3.766038000000	-1.146287000000
C	2.702407000000	-2.993081000000	-0.212705000000
C	3.508762000000	-1.911696000000	-0.167033000000
H	-3.216017000000	0.779106000000	-3.028282000000
H	-2.243462000000	-1.557240000000	-3.500700000000
H	-1.291506000000	-3.939434000000	-2.569494000000
H	0.832480000000	-4.683952000000	-1.456787000000
H	3.086281000000	-3.995080000000	-0.458623000000
H	4.585041000000	-1.986835000000	-0.387778000000
C	-1.426935000000	0.001707000000	4.519350000000
C	-2.321557000000	-0.557370000000	5.460127000000
H	-2.581577000000	-1.627481000000	5.404116000000
C	-2.897149000000	0.236526000000	6.464455000000
H	-3.591834000000	-0.211829000000	7.191276000000
C	-2.588199000000	1.606299000000	6.539147000000
H	-3.040209000000	2.229807000000	7.325812000000
C	-1.703398000000	2.178283000000	5.609310000000
H	-1.461245000000	3.250836000000	5.667758000000
C	-1.127142000000	1.380173000000	4.607370000000
H	-0.433133000000	1.826735000000	3.877059000000
C	0.712412000000	-2.209837000000	3.713821000000
C	0.447568000000	-3.440013000000	4.358167000000
H	-0.586477000000	-3.710627000000	4.626920000000
C	1.486757000000	-4.336513000000	4.657663000000
H	1.261896000000	-5.291561000000	5.157038000000
C	2.813517000000	-4.016664000000	4.319667000000
H	3.626034000000	-4.722611000000	4.550539000000
C	3.099586000000	-2.786150000000	3.704581000000
H	4.139313000000	-2.517879000000	3.460077000000
C	2.056743000000	-1.892069000000	3.412717000000
H	2.286030000000	-0.918694000000	2.952733000000
C	-2.022489000000	-2.064198000000	2.336854000000
C	-3.272173000000	-1.451771000000	2.078265000000
H	-3.446917000000	-0.417859000000	2.419500000000
C	-4.302470000000	-2.143570000000	1.419449000000
H	-5.266667000000	-1.646636000000	1.232029000000
C	-4.107963000000	-3.475887000000	1.016688000000
H	-4.918297000000	-4.023630000000	0.511892000000
C	-2.878908000000	-4.108275000000	1.270073000000
H	-2.724896000000	-5.155545000000	0.967496000000
C	-1.848212000000	-3.406735000000	1.920007000000
H	-0.897010000000	-3.919685000000	2.130776000000
C	1.571544000000	-0.232534000000	-4.074026000000
C	1.694952000000	-1.430729000000	-3.341278000000
H	1.416716000000	-1.437755000000	-2.275821000000
C	2.180765000000	-2.605142000000	-3.937425000000
H	2.279309000000	-3.526592000000	-3.343280000000
C	2.548909000000	-2.600290000000	-5.292851000000
H	2.931295000000	-3.517663000000	-5.765914000000
C	2.433765000000	-1.416272000000	-6.043228000000
H	2.725662000000	-1.407497000000	-7.104547000000

C	1.954410000000	-0.244118000000	-5.436515000000
H	1.887459000000	0.680970000000	-6.032652000000
C	2.293281000000	2.651984000000	-3.375713000000
C	3.629461000000	2.273625000000	-3.646061000000
H	3.858586000000	1.219202000000	-3.868740000000
C	4.672478000000	3.214154000000	-3.624356000000
H	5.705348000000	2.897326000000	-3.836483000000
C	4.395750000000	4.562810000000	-3.337851000000
H	5.209736000000	5.303505000000	-3.320830000000
C	3.070295000000	4.965145000000	-3.097059000000
H	2.844786000000	6.025173000000	-2.901165000000
C	2.032802000000	4.017602000000	-3.121362000000
H	1.001176000000	4.354158000000	-2.938927000000
C	-0.674839000000	1.898501000000	-4.018210000000
C	-1.394205000000	2.967759000000	-3.436563000000
H	-0.976647000000	3.489568000000	-2.561422000000
C	-2.650359000000	3.356568000000	-3.929682000000
H	-3.187947000000	4.200649000000	-3.470022000000
C	-3.222959000000	2.665752000000	-5.012565000000
H	-4.207741000000	2.965940000000	-5.402041000000
C	-2.525577000000	1.596097000000	-5.602864000000
H	-2.968118000000	1.055035000000	-6.453451000000
C	-1.262428000000	1.223149000000	-5.111920000000
H	-0.729621000000	0.379470000000	-5.578857000000

Input Files

DFT Optimisation

```
!BP86 def2-svp D3BJ opt numfreq slowconv

%pal
nprocs 32
end

%basis
newGTO O "def2-TZVP" end
newGTO Se "def2-TZVP" end
newGTO Cl "def2-TZVP" end
newgto Dy
 0 6
 1 1205955.486947000027 0.008165729207
 2 535980.216420999961 -0.004019299653
 3 238213.429520000005 0.016042861724
 4 105872.635341999994 0.006534642408
 5 47054.504596999999 0.032501357805
 6 20913.113153999999 0.044343203836
 0 1
 7 9294.716957000001 1.000000000000
 0 1
 8 4130.985314000000 1.000000000000
 0 1
```

SUPPORTING INFORMATION

9 1835.993473000000 1.000000000000
0 1
10 815.997099000000 1.000000000000
0 1
11 362.665377000000 1.000000000000
0 1
12 161.184612000000 1.000000000000
0 1
13 71.637605000000 1.000000000000
0 1
14 31.838936000000 1.000000000000
0 1
15 14.150638000000 1.000000000000
0 1
16 6.289172000000 1.000000000000
0 1
17 2.795188000000 1.000000000000
0 1
18 1.242306000000 1.000000000000
0 1
19 0.552136000000 1.000000000000
0 1
20 0.245394000000 1.000000000000
0 1
21 0.109064000000 1.000000000000
0 1
22 0.048473000000 1.000000000000
0 1
23 0.021543000000 1.000000000000
1 5
1 16500.520027999999 0.004760264705
2 6600.208011000000 0.005897483480
3 2640.083204000000 0.029326527847
4 1056.033282000000 0.089161858001
5 422.413313000000 0.265122289728
1 1
6 168.965325000000 1.000000000000
1 1
7 67.586130000000 1.000000000000
1 1
8 27.034452000000 1.000000000000
1 1
9 10.813781000000 1.000000000000
1 1
10 4.325512000000 1.000000000000
1 1
11 1.730205000000 1.000000000000
1 1
12 0.692082000000 1.000000000000
1 1
13 0.276833000000 1.000000000000
1 1
14 0.110733000000 1.000000000000
1 1
15 0.044293000000 1.000000000000
1 1
16 0.017717000000 1.000000000000
2 4
1 1185.048662000000 0.004734300415
2 430.926786000000 0.026490774838

```
  3 156.700650000000 0.145474353692
  4 56.982054000000 0.463452784138
  2 1
  5 20.720747000000 1.000000000000
  2 1
  6 7.534817000000 1.000000000000
  2 1
  7 2.739933000000 1.000000000000
  2 1
  8 0.996339000000 1.000000000000
  2 1
  9 0.362305000000 1.000000000000
  2 1
  10 0.131747000000 1.000000000000
  2 1
  11 0.047908000000 1.000000000000
  2 1
  12 0.017421000000 1.000000000000
  3 4
  1 33.836944000000 0.101241740066
  2 11.278981000000 0.330021330584
  3 3.759660000000 0.494377985697
  4 1.253220000000 0.347706969111
  3 1
  5 0.417740000000 0.145206846483
  3 1
  6 0.139247000000 1.000000000000
end
end

%scf
maxiter 8000
end

%scf
directresetfreq 1
diismaxeq 25
end

%method
SpecialGridAtoms 66
SpecialGridIntAcc 9
end

*xyz 1 6
Coordinates
*
```

EDA

```
#!/bin/sh

# dependency: D:/ADF_DATA/Dy-crown/O4Se2/DyO4Se2Cl2.Region_1
DyO4Se2Cl2.Region_1.results/adf.rkf Region_1.rkf
# dependency: D:/ADF_DATA/Dy-crown/O4Se2/DyO4Se2Cl2.Region_2
DyO4Se2Cl2.Region_2.results/adf.rkf Region_2.rkf

"$AMSBIN/ams" -n 12 << eor
```

SUPPORTING INFORMATION

```
Task SinglePoint
System
  Atoms
    Dy 0.0 0.0 0.0 region=Region_1 adf.f=Region_1
    Cl 0.0 0.0 2.544938 region=Region_1 adf.f=Region_1
    Cl -0.456727 0.128008 -2.495154 region=Region_1 adf.f=Region_1
    Se -3.326147 -0.105112 0.433413 region=Region_2 adf.f=Region_2
    Se -1.750915 2.825753 0.385092 region=Region_2 adf.f=Region_2
    Se 1.567185 2.932135 0.192987 region=Region_2 adf.f=Region_2
    Se 3.313157 0.102861 0.071358 region=Region_2 adf.f=Region_2
    C -3.935339 1.326733 -0.656815 region=Region_2 adf.f=Region_2
    C -3.297071 2.513961 -0.675809 region=Region_2 adf.f=Region_2
    C -0.867951 4.031686 -0.789529 region=Region_2 adf.f=Region_2
    C 0.476742 4.074136 -0.869073 region=Region_2 adf.f=Region_2
    C 2.99537 2.703486 -1.044171 region=Region_2 adf.f=Region_2
    C 3.702658 1.557514 -1.094199 region=Region_2 adf.f=Region_2
    H -4.848661 1.145611 -1.244907 region=Region_2 adf.f=Region_2
    H -3.659308 3.361084 -1.279292 region=Region_2 adf.f=Region_2
    H -1.508886 4.712617 -1.371362 region=Region_2 adf.f=Region_2
    H 1.00278 4.793832 -1.515894 region=Region_2 adf.f=Region_2
    H 3.238444 3.568345 -1.681409 region=Region_2 adf.f=Region_2
    H 4.559909 1.427178 -1.773303 region=Region_2 adf.f=Region_2
    Se -1.569922 -2.922757 0.317363 region=Region_2 adf.f=Region_2
    Se 1.74677 -2.832496 0.159832 region=Region_2 adf.f=Region_2
    C -3.834321 -1.538113 -0.706399 region=Region_2 adf.f=Region_2
    C -3.122134 -2.681823 -0.754071 region=Region_2 adf.f=Region_2
    C -0.60736 -4.067966 -0.857662 region=Region_2 adf.f=Region_2
    C 0.738327 -4.03165 -0.922116 region=Region_2 adf.f=Region_2
    C 3.172361 -2.506817 -1.059651 region=Region_2 adf.f=Region_2
    C 3.805878 -1.318078 -1.096578 region=Region_2 adf.f=Region_2
    H -4.751747 -1.396963 -1.299024 region=Region_2 adf.f=Region_2
    H -3.423622 -3.532851 -1.384718 region=Region_2 adf.f=Region_2
    H -1.201806 -4.78637 -1.443857 region=Region_2 adf.f=Region_2
    H 1.313318 -4.71919 -1.562299 region=Region_2 adf.f=Region_2
    H 3.479377 -3.352543 -1.695069 region=Region_2 adf.f=Region_2
    H 4.662288 -1.131476 -1.76358 region=Region_2 adf.f=Region_2
  End
  Charge 1.0
  BondOrders
    1 2 1.0
    1 3 1.0
    1 4 1.0
    1 5 1.0
    1 6 1.0
    1 7 1.0
    1 20 1.0
    1 21 1.0
    4 8 1.0
    4 22 1.0
    5 9 1.0
    5 10 1.0
    6 11 1.0
    6 12 1.0
    7 13 1.0
    7 27 1.0
    8 9 2.0
```

```
        8 14 1.0
        9 15 1.0
        10 11 2.0
        10 16 1.0
        11 17 1.0
        12 13 2.0
        12 18 1.0
        13 19 1.0
        20 23 1.0
        20 24 1.0
        21 25 1.0
        21 26 1.0
        22 23 2.0
        22 28 1.0
        23 29 1.0
        24 25 2.0
        24 30 1.0
        25 31 1.0
        26 27 2.0
        26 32 1.0
        27 33 1.0
    End
End

Engine ADF
    Basis
        Type DZP
        Core None
        PerAtomType Symbol=Dy File=ZORA/TZP/Dy
        PerAtomType Symbol=Cl File=ZORA/DZP/Cl
        PerAtomType Symbol=Se File=ZORA/DZP/Se
        PerAtomType Symbol=C File=ZORA/DZP/C
        PerAtomType Symbol=H File=ZORA/DZP/H
    End
    SpinPolarization 5.0
    Fragments
        Region_1 =/home/netweb/Dy-crown/O4Se2/DyO4Se2Cl2.Region_1/ams.results/adf.rkf
        Region_2 =/home/netweb/Dy-crown/O4Se2/DyO4Se2Cl2.Region_2/ams.results/adf.rkf
    End

    Save TAPE15
    Print ETSLOWDIN-Unrestricted
    Print NOCVHIRSHFELD
    XC
        Hybrid PBE0
        DISPERSION GRIMME3 BJDAMP
    End
    Symmetry NOSYM
    Unrestricted Yes
    BeckeGrid
        Quality Good
    End
    LOCORB
    END
    NumericalQuality Good
    FullFock Yes
```

```
   AOMat2File Yes
      SCF
      DIIS
      N 15
      Cyc 20
      End
      Mixing 0.015
      Mixing1 0.09
      Iterations 1000
   End
   UnrestrictedFragments Yes
   ETSNOCV
      Enabled Yes
   End
EndEngine
eor

# ============
# NBO Analysis
# ============

cp "${AMS_RESULTSDIR-${AMS_JOBNAME-ams}.results}/adf.rkf" TAPE21
cp "${AMS_RESULTSDIR-${AMS_JOBNAME-ams}.results}/TAPE15" TAPE15
"$AMSBIN/adfnbo" << eor
write
spherical
eor

"$AMSBIN/gennbo6" FILE47

"$AMSBIN/adfnbo" << eor
spherical
fock
read
eor

mv TAPE21 "${AMS_RESULTSDIR-${AMS_JOBNAME-ams}.results}/adf.rkf"
rm -f TAPE15
```

CASSCF

```
!DKH2 DKH-def2-svp slowconv tightscf autoaux nofrozencore
!moread
%moinp " OSe-Cl-c.gbw"

%pal nprocs 12
end

%Maxcore 6000

%basis
newGTO O "DKH-def2-TZVP" end
newGTO Se "DKH-def2-TZVP" end
newGTO Cl "DKH-def2-TZVP" end
newgto Dy
```

SUPPORTING INFORMATION

0 6
1 1205955.486947000027 0.008165729207
2 535980.216420999961 -0.004019299653
3 238213.429520000005 0.016042861724
4 105872.635341999994 0.006534642408
5 47054.504596999999 0.032501357805
6 20913.113153999999 0.044343203836
0 1
7 9294.716957000001 1.000000000000
0 1
8 4130.985314000000 1.000000000000
0 1
9 1835.993473000000 1.000000000000
0 1
10 815.997099000000 1.000000000000
0 1
11 362.665377000000 1.000000000000
0 1
12 161.184612000000 1.000000000000
0 1
13 71.637605000000 1.000000000000
0 1
14 31.838936000000 1.000000000000
0 1
15 14.150638000000 1.000000000000
0 1
16 6.289172000000 1.000000000000
0 1
17 2.795188000000 1.000000000000
0 1
18 1.242306000000 1.000000000000
0 1
19 0.552136000000 1.000000000000
0 1
20 0.245394000000 1.000000000000
0 1
21 0.109064000000 1.000000000000
0 1
22 0.048473000000 1.000000000000
0 1
23 0.021543000000 1.000000000000
1 5
1 16500.520027999999 0.004760264705
2 6600.208011000000 0.005897483480
3 2640.083204000000 0.029326527847
4 1056.033282000000 0.089161858001
5 422.413313000000 0.265122289728
1 1
6 168.965325000000 1.000000000000
1 1
7 67.586130000000 1.000000000000
1 1
8 27.034452000000 1.000000000000
1 1
9 10.813781000000 1.000000000000
1 1

```
  10 4.325512000000 1.000000000000
  1 1
  11 1.730205000000 1.000000000000
  1 1
  12 0.692082000000 1.000000000000
  1 1
  13 0.276833000000 1.000000000000
  1 1
  14 0.110733000000 1.000000000000
  1 1
  15 0.044293000000 1.000000000000
  1 1
  16 0.017717000000 1.000000000000
  2 4
  1 1185.048662000000 0.004734300415
  2 430.926786000000 0.026490774838
  3 156.700650000000 0.145474353692
  4 56.982054000000 0.463452784138
  2 1
  5 20.720747000000 1.000000000000
  2 1
  6 7.534817000000 1.000000000000
  2 1
  7 2.739933000000 1.000000000000
  2 1
  8 0.996339000000 1.000000000000
  2 1
  9 0.362305000000 1.000000000000
  2 1
  10 0.131747000000 1.000000000000
  2 1
  11 0.047908000000 1.000000000000
  2 1
  12 0.017421000000 1.000000000000
  3 4
  1 33.836944000000 0.101241740066
  2 11.278981000000 0.330021330584
  3 3.759660000000 0.494377985697
  4 1.253220000000 0.347706969111
  3 1
  5 0.417740000000 0.145206846483
  3 1
  6 0.139247000000 1.000000000000
end
end

%method
SpecialGridAtoms 66
SpecialGridIntAcc 9
end

%casscf
nel 9
norb 7
mult 6,4
nroots 21,224
```

```
actorbs forbs
maxiter 100
ci
nguessmat 8000
maxiter 100
end

rel
dosoc true
gtensor true
printlevel 3
NDoubGTensor 8
domagnetization true
dosusceptibility true
end

ANISO
doaniso true
MLTP 2,2,2,2,2,2,2,2
TINT 0, 300, 100
HINT 0, 7.0, 10
TMAG 2.0, 3.0, 5.0
CRYS_element "Dy"
CRYS_charge 3
PLOT true
UBAR true
end
end

*xyz 1 6
Coordinates
*
```

References

1 F. Neese, *WIREs Comput. Mol. Sci.*, 2022, **12**, e1606.
2 A. D. Becke, *J. Chem. Phys.*, 1993, **98**, 5648–5652.
3 J. P. Perdew, J. Tao, V. N. Staroverov and G. E. Scuseria, *J. Chem. Phys.*, 2004, **120**, 6898–6911.
4 S. Grimme, S. Ehrlich and L. Goerigk, *J. Comput. Chem.*, 2011, **32**, 1456–1465.
5 D. Aravena, M. Atanasov and F. Neese, *Inorg. Chem.*, 2016, **55**, 4457–4469.
6 I. Tarannum, S. Moorthy and S. K. Singh, *Dalton Trans.*, 2023, **52**, 15576–15589.
7 S. K. Singh, C. J. Cramer and L. Gagliardi, *Inorg. Chem.*, 2020, **59**, 6815–6825.
8 D. Ray, M. S. Oakley, A. Sarkar, X. Bai and L. Gagliardi, *Inorg. Chem.*, 2023, **62**, 1649–1658.
9 T. Noro, M. Sekiya and T. Koga, *Theor. Chem. Acc.*, 2012, **131**, 1124.
10 F. Weigend and R. Ahlrichs, *Phys. Chem. Chem. Phys.*, 2005, **7**, 3297–3305.
11 P. Pracht, F. Bohle and S. Grimme, *Phys. Chem. Chem. Phys.*, 2020, **22**, 7169–7192.
12 C. Adamo and V. Barone, *J. Chem. Phys.*, 1999, **110**, 6158–6170.

13 E. D. Glendening, C. R. Landis and F. Weinhold, *J. Comput. Chem.*, 2013, **34**, 1429–1437.
14 B. O. Roos, P. R. Taylor and P. E. M. Sigbahn, *Chem. Phys.*, 1980, **48**, 157–173.
15 D. A. Pantazis and F. Neese, *J. Chem. Theory Comput.*, 2009, **5**, 2229–2238.
16 M. Atanasov, D. Ganyushin, K. Sivalingam and F. Neese, in *Molecular Electronic Structures of Transition Metal Complexes II*, eds. D. M. P. Mingos, P. Day and J. P. Dahl, Springer, Berlin, Heidelberg, 2012, pp. 149–220.
17 D. Aravena, *J. Phys. Chem. Lett.*, 2018, **9**, 5327–5333.
18 A. Castro-Alvarez, Y. Gil, L. Llanos and D. Aravena, *Inorg. Chem. Front.*, 2020, **7**, 2478–2486.
19 L. Ungur, M. Thewissen, J.-P. Costes, W. Wernsdorfer and L. F. Chibotaru, *Inorg. Chem.*, 2013, **52**, 6328–6337.
20 A. B. Canaj, S. Dey, E. R. Martí, C. Wilson, G. Rajaraman and M. Murrie, *Angew. Chem. Int. Ed.*, 2019, **58**, 14146–14151.
21 Z.-H. Li, Y.-Q. Zhai, W.-P. Chen, Y.-S. Ding and Y.-Z. Zheng, *Chem. – Eur. J.*, 2019, **25**, 16219–16224.
[22] Z. Zhu, C. Zhao, Q. Zhou, S. Liu, X.-L. Li, A. Mansikkam, J. Tang, *CCS Chem.* **2022**, *4*, 3762–3771.
23 S. Liu, Y. Gil, C. Zhao, J. Wu, Z. Zhu, X.-L. Li, D. Aravena and J. Tang, *Inorg. Chem. Front.*, 2022, **9**, 4982–4989.
24 X.-L. Ding, Y.-Q. Zhai, T. Han, W.-P. Chen, Y.-S. Ding and Y.-Z. Zheng, *Chem. – Eur. J.*, 2021, **27**, 2623–2627.
25 Y. Ding, N. F. Chilton, R. E. P. Winpenny and Y. Zheng, *Angew. Chem. Int. Ed.*, 2016, **55**, 16071–16074.
26 L. Maxwell, M. Amoza and E. Ruiz, *Inorg. Chem.*, 2018, **57**, 13225–13234.
27 P. Kalita, N. Ahmed, S. Moorthy, V. Béreau, A. K. Bar, P. Kumar, P. Nayak, J.-P. Sutter, S. K. Singh and V. Chandrasekhar, *Dalton Trans.*, 2023, **52**, 2804–2815.
28 X. Ding, Y. Zhai, T. Han, W. Chen, Y. Ding and Y. Zheng, *Chem. – Eur. J.*, 2021, **27**, 2623–2627.
29 X. Meng, M. Wang, X. Gou, W. Lan, K. Jia, Y.-X. Wang, Y.-Q. Zhang, W. Shi and P. Cheng, *Inorg. Chem. Front.*, 2021, **8**, 2349–2355.
30 S. Bala, G.-Z. Huang, Z.-Y. Ruan, S.-G. Wu, Y. Liu, L.-F. Wang, J.-L. Liu and M.-L. Tong, *Chem. Commun.*, 2019, **55**, 9939–9942.
31 Y.-S. Ding, W. J. A. Blackmore, Y.-Q. Zhai, M. J. Giansiracusa, D. Reta, I. Vitorica-Yrezabal, R. E. P. Winpenny, N. F. Chilton and Y.-Z. Zheng, *Inorg. Chem.*, 2022, **61**, 227–235.
32 A. B. Canaj, S. Dey, E. R. Martí, C. Wilson, G. Rajaraman and M. Murrie, *Angew. Chem. Int. Ed.*, 2019, **58**, 14146–14151.
33 Z. Zhu, C. Zhao, T. Feng, X. Liu, X. Ying, X.-L. Li, Y.-Q. Zhang and J. Tang, *J. Am. Chem. Soc.*, 2021, **143**, 10077–10082.
34 S.-D. Jiang, B.-W. Wang, G. Su, Z.-M. Wang and S. Gao, *Angew. Chem. Int. Ed.*, 2010, **49**, 7448–7451.
35 Y. Wang, X.-L. Li, T.-W. Wang, Y. Song and X.-Z. You, *Inorg. Chem.*, 2010, **49**, 969–976.